Progress in Aerospace Sciences 137 (2023) 100887

Contents lists available at ScienceDirect

Progress in Aerospace Sciences

journal homepage: www.elsevier.com/locate/paerosci

Review of rotating wing dynamic stall: Experiments and flow control

Anthony D. Gardner [a], Anya R. Jones [b], Karen Mulleners [c], Jonathan W. Naughton [d], Marilyn J. Smith [e,*]

[a] German Aerospace Center (DLR), Göttingen, Germany
[b] University of Maryland, College Park, MD, USA
[c] Swiss Federal Institute of Technology, Lausanne, Switzerland
[d] University of Wyoming, Laramie, WY, USA
[e] Georgia Institute of Technology, Atlanta, GA, USA

ARTICLE INFO

Keywords:
Vertical lift
Dynamic stall
Experiments
Flow control
Measurement techniques
Review article

ABSTRACT

Dynamic stall has been a technical challenge and a fluid dynamical subject of interest for more than fifty years; but in the last decade significant advances have been made in the understanding, prediction, modeling, and control of dynamic stall on rotors. This paper provides a summary of the state of the art of dynamic stall experiments and future directions in the understanding of dynamic stall on rotors. Experimental data sets are discussed, as well the direction of future research for control of dynamic stall. Coordinated testing between airfoils and rotating blades, as well as close integration between computational and experimental studies were found to be productive approaches. Advanced analysis methods, including statistical methods, modal representations, and artificial intelligence methods have led to significant advances in the understanding of dynamic stall. Investigations of dynamic stall control devices have allowed many useful targeted investigations of the transition to separated flow, but have not yet resulted in a commercially implemented device.

1. Introduction

Classic dynamic stall is an unsteady aerodynamic phenomenon resulting from the combination of high angles of attack and a rapid angle of attack change of a lifting surface during which the flow separates. In practice, dynamic stall is generated by complex flowfield phenomena including shear layers and vortices that interact with one another [1]. Dynamic stall is classically of primary interest in rotor aerodynamics, but is a key element of many problems in unsteady aerodynamics including fixed and flapping wing vehicles, axial and cross-flow wind and tidal turbines, and flight through air wakes. The ability to predict dynamic stall and mitigate it within flight envelopes of many scales is necessary to improve current safety standards and to mitigate the effects of dynamic stall in new designs and missions. Dynamic stall has been studied for more than fifty years. However, driven by advances in computational modeling and optical measurement techniques over the last decade, significant advances have been accomplished in the understanding, prediction, modeling and control of dynamic stall in many applications, most notably on rotating wings. This is visible in the large number of publications on both translating and rotating wing dynamic stall (~19,000 since 1970) as illustrated in Fig. 1.

Research in dynamic stall continues to achieve improved accuracy in quantitative predictions to inform new rotor designs needed for future military [2,3] or civil helicopters [4]. Dynamic stall is an important load case that limits the dimensions of new helicopters, so increased accuracy in the predictions of loads will improve the structural design of future vehicles. The ability to predict and control dynamic stall is also necessary to improve upon current safety standards, and an improved understanding of the physics of dynamic stall and resulting blade loads will provide better estimates of achievable flight envelopes. This is true for existing vehicles and missions, as well as for future Urban Air Mobility (UAM) applications, where flight in urban and unsteady aerodynamic environments can result in additional sources of rapid changes in blade angle of attack (thereby risking dynamic stall) due to flight through wakes and gusts [5,6].

Dynamic stall behavior in rotating wing applications is dependent on a large variety of conditions, and its complex and nonlinear behavior has been the focus of many experimental and computational efforts. Current lower fidelity numerical analysis is insufficient for capturing the details of dynamic stall [3], so computational fluid dynamics (CFD) or computational fluid dynamics-computational structural dynamics (CFD-CSD) analyses are desirable [7]. Experiments in dynamic

* Corresponding author.
E-mail addresses: tony.gardner@dlr.de (A.D. Gardner), arjones@umd.edu (A.R. Jones), karen.mulleners@epfl.ch (K. Mulleners), naughton@uwyo.edu (J.W. Naughton), ms55@gatech.edu (M.J. Smith).

https://doi.org/10.1016/j.paerosci.2023.100887
Received 10 October 2022; Received in revised form 14 January 2023; Accepted 14 January 2023
Available online 4 February 2023

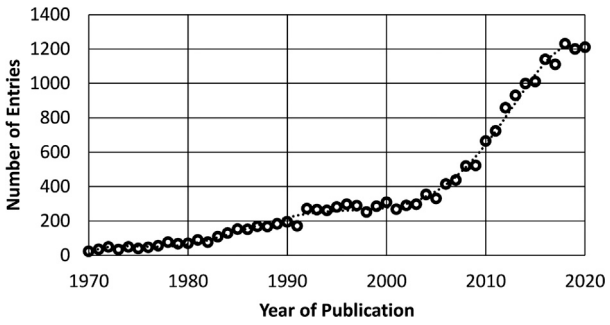

Fig. 1. Google Scholar entries for "dynamic stall", by year.

stall largely fall into two categories: the investigation of the physical phenomena associated with dynamic stall and the development of databases for high-fidelity computational validation. These experiments are of course not mutually exclusive, but experiments are typically designed in the first instance with a focus towards one or the other. Since the advent of high-fidelity, first-principles modeling in the design of experiments, significant advances in the quality of the experiments have been made, particularly in the selection of sensor positioning and in the understanding of how the discrete sensor positioning affects the comparisons between experiments and CFD [8]. CFD computations of experimental geometries and conditions have also clarified previously under-explored systematic errors that can arise due to model mounting and wind tunnel interference, resulting in a reevaluation of how experiments and CFD can complement each other in the development of our understanding of dynamic stall and other complex aerodynamic phenomena.

Dynamic stall experiments have been performed on many different apparatuses, ranging from those that isolate specific phenomena to those that capture a wide range of phenomenon. Flight tests, for example, promise a full range of aerodynamic phenomena, but are costly and limited in the measurement techniques and resolution available and in the part of the flight envelope they can cover, so that identification and analysis of the stall phenomena are hindered. Rotor test rigs allow additional measurement techniques, but the flexible surfaces in a rotating system and the requirement of a large wind tunnel typically limit the range of measurements that can reasonably be performed. Furthermore, even when high quality measurements can be acquired, it can be difficult to separate the causes of load and flow phenomena due to the complex environment. Further reductions in the physical complexity of the experimental apparatus (finite wings, pitching airfoils) can allow more detailed understanding of the individual dynamic stall phenomena, typically with increased measurement resolution. Finally, more canonical experiments and a direct comparison with classic theory can form a strong theoretical foundation for understanding the more complex flows that evolve on rotors in flight.

The improved understanding of dynamic stall through experiments and computations can guide new ideas to control these flows. A wide array of flow control experiments for dynamic stall are reviewed here, showing the strengths of different approaches. Many passive and active flow control strategies have been demonstrated to be effective in suppressing or delaying dynamic stall in a controlled experimental or numerical setting. These proof of concept experiments contribute to our understanding of the development of dynamic stall even if the tested approaches have not made to the implementation stage yet.

The remainder of this article is arranged as follows. Section 2 provides a description of dynamic stall followed by a description of different experiments including those conducted in flight (Section 3.1), on rotor rigs (Section 3.2), on pitching wings (Section 3.3), and on airfoils (Section 3.4) as well as specialized experiments to address particular phenomena (Section 3.5). Special topics related to dynamic stall measurement are presented in Section 4. Following these experiments, a discussion of control of dynamic stall is presented in Section 5. Finally, future directions and concluding remarks are presented in Section 6.

This review article is focused primarily on experimental advances in state of the art in rotating dynamic stall. Advances in this field require experimental, computational and theoretical contributions that together provide a full overview of the field. Additional topics not covered by this paper include aeroelastic modeling of dynamic stall on rotors and sensing of the onset of dynamic stall, among other areas that focus on more traditional computational and theoretical advances.

2. Definition of dynamic stall

Classically, dynamic stall has been defined as the unsteady phenomenon when flow separates then reattaches as the pitch angle (angle of attack) harmonically oscillates on a lifting surface such as a wing or rotor blade. In many cases (e.g., on a rotor in forward flight), the angle of attack of the blade varies periodically with a large amplitude, and thus subsequent to dynamic stall, the blade pitches down and flow reattaches [9]. Many of the examples that follow will be in-line with that concept.

For the purposes of this review, dynamic stall has been generalized to be the process of unsteady flow separation on a lifting surface at an effective angle of attack greater than the static stall angle. Flow separation, and thus stall, can be delayed due to rapid increases in the effective angle of attack of the surface (i.e., wing, blade, or plate) due to either changes in blade pitch (i.e., motion of the blade) or in the relative flow speed and/or direction (e.g., gust encounters or blade-vortex interactions). Flow reattachment is a complex process that has attracted much research in its own right [10–13], and thus for the purposes of the current work, the following sections will focus primarily on the process of flow separation and stall (and the resulting flow phenomena and blade loading) rather than reattachment and recovery.

Over the years, dynamic stall has often been categorized in a number of ways. One of the more common is to differentiate between *light* and *deep* dynamic stall [1]. These descriptors are typically used to emphasize the "amount" of stall. In general if a pitching airfoil is driven in a high amplitude pitch variation (Fig. 2), there will be some range of angles of attack over which dynamic stall first occurs and where increasing amplitude results in increasing pitching moment peaks. This "light stall" region is also relatively sensitive to small changes in the input conditions. If the amplitude is further increased, the forces caused by stall no longer continue to increase, and the aerodynamics become relatively insensitive to small changes in the input conditions. This "deep stall" region typically does not have a clear separation from that of "light dynamic stall", and the definitions of the bounds vary in the literature. Most classifications are based on the degree and extent of the flow separation. A distinction based on underlying physical mechanism and timing of stall onset is proposed by [14]. When the onset of dynamic stall on an oscillating airfoil occurs before the maximum angle of attack is reached, the flow and force responses show the general features of deep dynamic stall. Conditions where the sign of the pitch rate is reversed before the dynamic stall onset angle of attack is reached, are considered light dynamic stall conditions.

Similarly, *trailing edge stall* and *leading edge stall* are used to describe the progression of dynamic stall [16]. Pitching thick airfoils (or sometimes thin airfoils if the pitch rate is sufficiently slow) typically display a separation region that grows from the trailing edge towards the leading edge. This results in a relatively gentle peak in lift before stall occurs, as illustrated in Fig. 3. This "trailing edge stall" can be contrasted with "leading edge stall", in which the separation region grows from the leading edge, while the flow near the trailing edge remains (temporarily) attached. In this case, which occurs for thin airfoils, airfoils with sharper leading edges, or airfoils that are pitched more rapidly, flow separation occurs within a short time and leads to

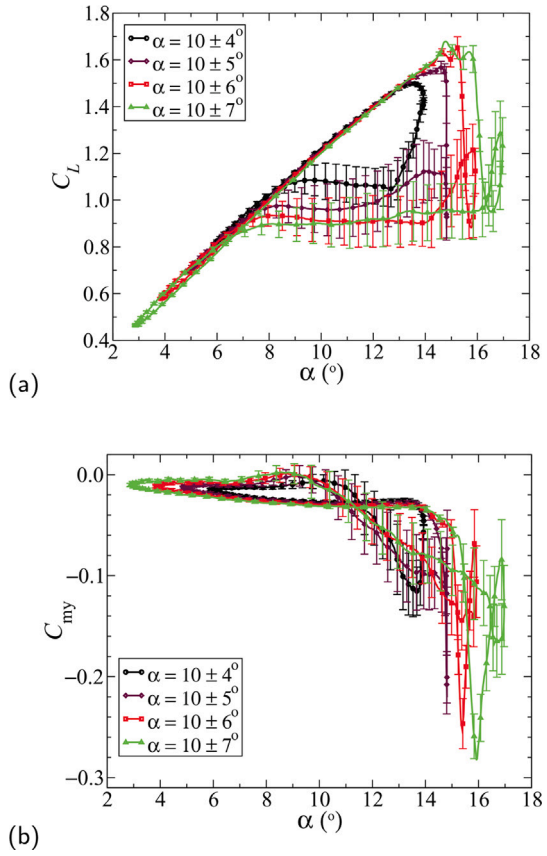

Fig. 2. Dynamic stall of the EDI-M109 airfoil at Mach 0.3 showing increasing pitching moment peaks with increasing pitching amplitude. [15]. (a) Lift (b) Pitching moment.

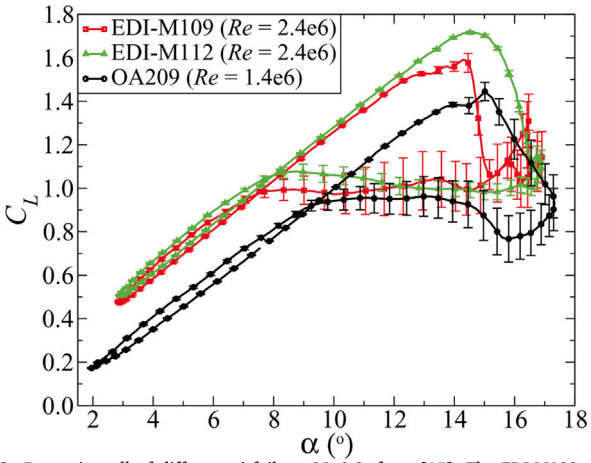

Fig. 3. Dynamic stall of different airfoils at M=0.3, from [15]. The EDI-M109 airfoil shows a lift history typical of leading edge stall, whereas the EDI-M112 shows a lift history typical of trailing edge stall. The OA209 airfoil has been shown by PIV measurements to have leading edge stall [14], but the lift history is intermediate between the other two.

a more sudden stall. *Reverse flow* dynamic stall is a relatively rare phenomena that occurs on rotors operating at high advance ratio. In this case, the relative freestream moves from the typically sharp geometric trailing edge of the blade to the typically blunt geometric leading edge. In reverse flow, the sharp aerodynamic leading edge typically leads to rapid flow separation and thus leading edge stall [17–20].

Dynamic stall can occur anywhere along the rotor radius, so that the local freestream Mach number may vary from incompressible to high subsonic compressible. Compressibility effects, which may be found in freestream velocities as low as $M_\infty = 0.2$, have been observed to change the mechanism of dynamic stall, as well as reduce the nonlinear lift peaks at onset of dynamic stall, when compared to their incompressible counterparts. Carr and Chandrasekhara [21] have published a review of compressibility on dynamic stall that further elucidates these effects.

If a rotor blade moves through a wake, region of vortices (e.g., shed from preceding blades), or turbulent air, the aerodynamic angle of attack may suddenly change due to the ambient environment rather than any particular motion of the blade itself. In these cases of *wake ingestion* or *blade-vortex interaction*, dynamic stall may occur even though the physical angle of attack is relatively constant [22]. This type of interaction is relatively common for highly loaded rotors or rotors in turning flight, and is also a primary cause of structural loads and acoustic emissions.

These terms form a basis for a common language that will be used to discuss the characteristic flow phenomena and the associated force responses in the following examples, which range from three-dimensional, high Reynolds number flight tests, to nominally two-dimensional low Reynolds number pitching airfoils.

3. Dynamic stall experiments

3.1. Flight tests

The most direct method of measuring a flight-relevant flow is to instrument a flight vehicle. Flight tests can provide invaluable data, but at high cost and typically lower measurement resolution than is possible in the laboratory. The most complete set of dynamic stall flight data comes from the NASA UH-60 (Fig. 4a) flight program [23]. In this program, the UH-60 helicopter was instrumented with 242 pressure sensors, which could be individually analyzed or integrated, and dynamic stall detection was provided by pressure sensor analysis (Fig. 5). Dynamic stall was observed in level flight corresponding to the advance ratio μ=0.3 and solidity-weighted thrust C_T/σ=0.12 case. Dynamic stall was also observed in a pull-up maneuver. Stall regions are highlighted in Fig. 5 on the retreating blade side of the rotor disk (third and fourth quadrants), and also in the first quadrant for some flight conditions. These data confirm results from flexible rotor wind tunnel tests and their corresponding computations (e.g., on the 7 A [24] and UH-60 A [25] rotors). In an operational flight environment, at least three stall events from different origins can occur during a single blade revolution.

In a separate flight test, a dynamic stall point was also observed on the Bluecopter helicopter (Fig. 4b) during strong left turning flight [4]. The rotor advance ratio at this point was μ=0.35 and the descent angle was 9°. Based on the available instrumentation and sensor data, a rotor thrust coefficient of C_T/σ=0.145 was computed with 5% accuracy. The helicopter was only instrumented with control settings, attitude and flight speed, pitch link loads and rotor thrust instrumentation, and flow measurements of dynamic stall are not available.

Flight test data provide a rich source of data on the possible ramifications of dynamic stall, particularly on vibration and structural loads. Flight tests are not ideal to identify the aerodynamic sources of the loads or to validate computational methods. Measurements during flight tests are typically restricted by safety considerations and by the limitations of instrumenting a certified aircraft. Tests on isolated rotors provide more insights into the aerodynamics of a rotor, with fewer test restrictions.

3.2. Rotor test rigs

Dynamic stall can be triggered not only by high angles of attack, but also by blade-vortex interactions, shocks, and rotor trim to high collective pitch. The primary differences in the dynamic stall vortex on a rotor (rather than a non-rotating airfoil) are that the vortex is more compact and that the rotational motion of the rotor has a stabilizing effect on its formation and convection [27]. As such, it is useful to move from flight tests to stationary rotors, decreasing the complexity of the flow while maintaining blade rotation, before simplifying the flow.

Fig. 4. (a) NASA UH-60 aircraft. [26] (b) Bluecopter demonstrator helicopter, from [4].

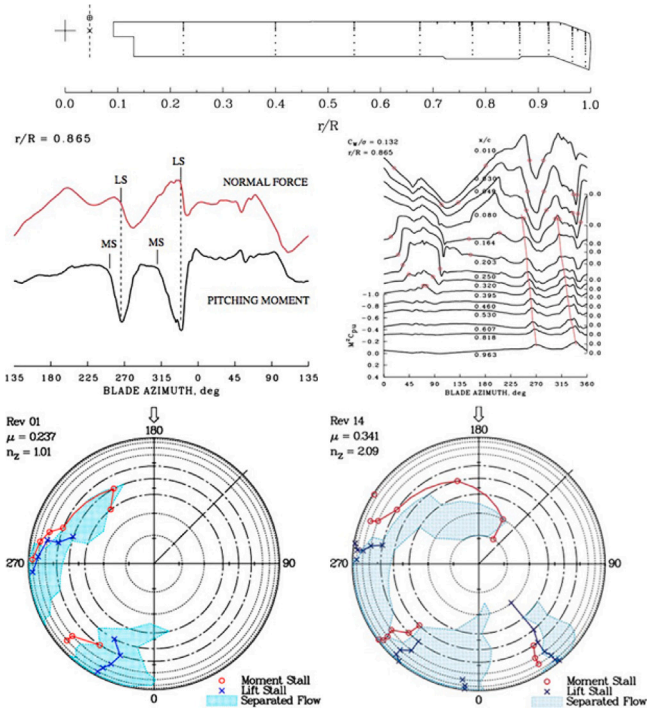

Fig. 5. Images from UH-60 airloads program tutorial [26].

3.2.1. Flexible rotors

The consequences of dynamic stall can include strong aerodynamic flutter and the typical double-hump local aerodynamic angle of attack progressions. On flexible rotors, the angle of the rotor blade increases until dynamic stall occurs. The resulting high negative pitching moment then causes a nose-down torsion of the blade tip (although the root is still increasing in pitch angle). When the negative pitching moment peak drops off, often with partial flow reattachment, the blade springs back to higher angles of attack, causing a second stall. Thus the blade

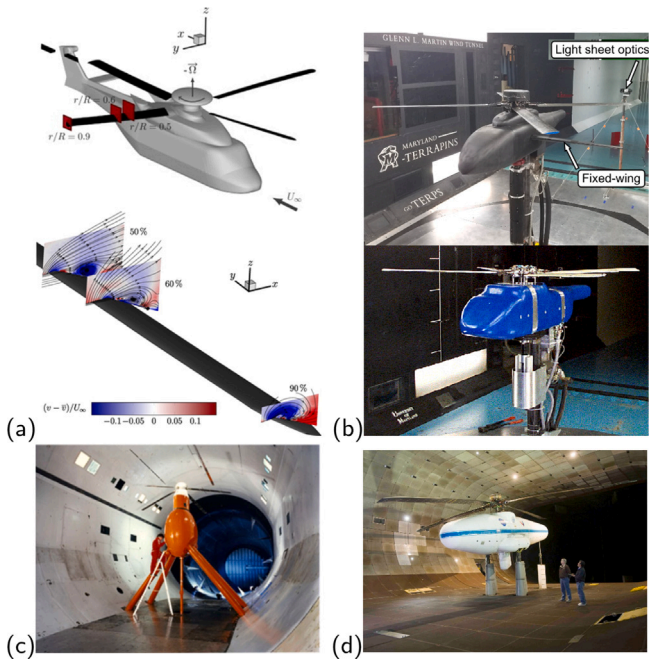

Fig. 6. Examples of flexible rotor wind tunnel experiments. (a) GOAHEAD [27] (b) University of Maryland (UMD) rotor stand in the Glenn L. Martin Wind Tunnel (GLMWT) [28,29] (c) Onera 7AD rotor in SM1 A wind tunnel [24] (d) Tunnel test of the UH-60 A airloads rotor [30].

motion is not a function similar to a sine-wave, but rather a double-hump near the peak angle of attack. This is common for all rotors with deep dynamic stall, but has clearly been observed on the UH-60 A and 7AD [25,31].

Since the blade elasticity can lead directly to stall, it is one of the most important differences between stiff and flexible rotors. A complete set of measurement of the flight conditions, blade shapes, and structural properties during a flexible rotor experiment are desirable for high-fidelity computational validations. Experimental campaigns of these rotors therefore require more instrumentation than their stiff rotor counterparts to accurately quantify both the aerodynamic and structural loads, as well as blade deflections. Some datasets on flexible rotors include those represented in Fig. 6: the GOAHEAD project data, acquired for only a relatively small number of cycles [32]; the 7A/7D internal ONERA data, some of which is published in Crozier [33]; the UH60 A data acquired over a large text matrix including a thrust and speed sweep [30]; and the UMD GLMWT data (e.g., [34]) which includes studies on several different configurations and, notably, time-resolved flowfield measurements in reverse flow dynamic stall [18].

High advance ratio rotors experience dynamic stall on the retreating side of the rotor disk in reverse flow. The loads generated by the stall in reversed flow are at low dynamic pressure, meaning that their impact on pitch link loads may be minimal in terms of pitching moment; however their impact on radial forces and drag can be important—especially when coupled to a lag damper or a rigid rotor with pitch/flap coupling.

Flexible rotor test data provide many of the same dynamic stall effects seen in flight. The measurements are restricted by safety considerations limiting the load on the rotors, and it is difficult to separate aeroelastic and trim effects from aerodynamic effects. Tests on stiff rotors can provide more insights into the aerodynamics with fewer dynamic effects.

3.2.2. Elastically stiff rotors

To produce an experiment which can be well reproduced computationally, the elastically stiff rotor offers a valuable compromise

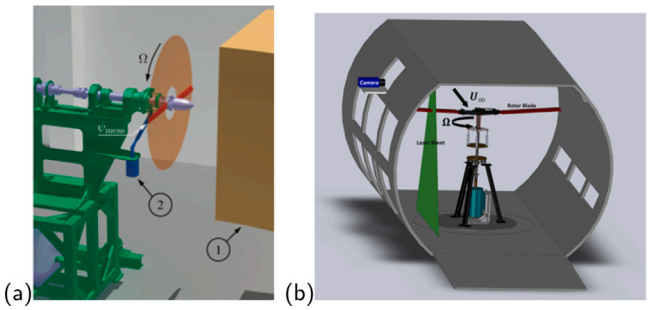

Fig. 7. Examples of stiff rotor experiments. (a) DLR Rotor Test stand Göttingen (RTG) [35] (b) Georgia Tech High Advance Ratio Facility (HARF) [36].

between the stiff finite wing and the flexible rotor. These tests are complex experiments that are often not directly related to industrial configurations, but are capable of generating high quality data for computational validation. Small-scale stiff rotors offer simplicity due to the ability to identify the rotor blades using known (prescribed) motion. In addition, these tests may be defined to explore deep dynamic stall, which is more difficult to achieve in flexible rotor tests. It remains challenging to obtain highly resolved flow field measurements due the rotating system transformations that make the three-dimensional flow difficult to visualize. Additionally, many small rotating wing experiments have low aspect ratios, low Reynolds numbers (and often low Mach numbers) with hubs and mounts that are bulky compared to their full-size counterparts. Alternatively, flexible rotors in the wind tunnel offer much more realistic aspect ratios and slender blades that operate at higher Mach and Reynolds numbers.

Notable stiff rotor test rigs include the DLR RTG axial inflow facility [35], Georgia Tech high advance ratio facility [36], Technical University of Munich Rotor [37], DLR wind tunnel rotor (GHM), and the NREL Phase VI [38] and Mexico [39]. Note that with the exception of the NREL facilities (for wind turbines), all of these rigs were designed, built, and operated with the purpose of modeling aerodynamics related to the operational envelope of a helicopter.

Two main approaches are typically employed in stiff rotor experiments, illustrated in Fig. 7. The RTG uses slow (<5 m/s) axial inflow from a wind tunnel to produce an effect similar to a pitching airfoil in the rotating system. In this setup, the blade Mach number is only a function of the rotor radius, much like a rotor in hover. The blade angle of attack is a function of the azimuthal position and varies periodically with the rotor frequency. This results in a flow situation where extensive data can be acquired for both stalled and fully attached flows at relatively low cost [35,40]. The Georgia Tech High Advance Ratio Facility (HARF), for example, employs a traditional closed circuit wind tunnel with a stiff rotor mounted normal to the flow direction to investigate rotors at varying advance ratios with dynamic stall [36].

Elastically stiff rotor test data allow researchers to isolate the aerodynamic effects from the elastic and dynamic effects of stall. Measurements are less restricted by safety considerations and high loads in deep dynamic stall can be achieved. However, results are restricted by the limitations of instrumenting the full rotor plane, and by the difficulty of achieving a high-quality inflow. The coupling effect of the rotor downwash hampers the extraction of the exact local aerodynamic angle of attack. Tests on pitching finite wings promise more insights into the unsteady and separating flow aerodynamics without the complexity of the rotating system.

3.3. Pitching finite wings

The finite wing (see Fig. 8 for examples) has long been a staple of aerodynamic research because it is a simple geometry that produces a three-dimensional flow and acts as an intermediate case study between airfoils and rotating wings. Attached to a pitching rig, it produces a relatively simple non-rotating three-dimensional flow that can be used for dynamic stall research. Early examples including [41] and [42], evaluated untwisted wings of constant cross section in an effort to maintain a simple geometry. Lorber's efforts included sweep to introduce a spanwise flow component during stall complementary to radial flows for rotating wings. This approach is practical for a numerical approach where an Euler wall can be applied at the attaching end, but experimentally this results in the initial dynamic stall appearing at the junction between the wind tunnel wall and the wing, with a correspondingly strong interaction between the two [43]. Alternative setups have applied positive twist and a range of airfoils [44,45] to move the point of initial stall outboard, creating aerodynamics that are more easily computed with numerical methods without considering the complete wind tunnel [46].

Dynamic stall on a three-dimensional wing (Fig. 9) typically results in a horseshoe-shaped Ω-vortex, which propagates downstream at different rates depending on its position. Although many investigations of this vortex have been performed on wings of relatively low aspect ratio where for static stall only a single stall cell is to be expected, Merz et al. [44] noted that the stall cells seen for static stall or slow pitch ramps correspond to separate Ω vortices during dynamic stall, and that these are the stall cells reported by Piziali [42] from surface flow visualization, and by Dell'Orso and Amitay [47] using fluorescent oil on static wings. Of relevance to rotating wings is the discovery that the dynamic stall on large portions of the finite wing produces force time histories qualitatively similar to those observed in two-dimensional experiments [41]. Since the physical mechanisms are different, measurements of only integral forces may result in erroneous conclusions [48]. From experiments with a swept finite wing, the effect of sweep is to delay stall to a higher angle of attack and to increase the maximum (sweep-angle normalized) lift for both static polars and dynamic stall [41,49].

Finite pitching wing test data allow researchers to separate the 3D aerodynamic stall effects from the effects of the rotor downwash. High loads can be achieved, and the 3D flow field can at least partially be resolved by measurements in multiple planes. Wing elasticity, and the effects of twist, taper and an anhedral angle make the results difficult to generalize. Tests on pitching airfoils promise more insights into the 2D aerodynamics, without the complexity of the 3D geometry.

3.4. Pitching airfoils

A large class of experiments address the two-dimensional pitching airfoil problem, of which perhaps the best known are the early experiments of McCroskey et al. [1]. The initial motivation for the work of McCroskey, et al. was guided by the dynamic stall problem on helicopter rotors. The angle of attack variation of a helicopter rotor blade during the rotation was measured experimentally by McCroskey and Fisher [9] for a helicopter in forward flight. The angle of attack variation during the part of the blade rotation where the rotor experiences dynamic stall is well represented by a sinusoidal oscillation with a large mean angle of attack, a large amplitude, and a pitching frequency equal to the fundamental rotor frequency. As a result, dynamic stall is often studied using a two-dimensional sinusoidally oscillating airfoil [1,14,17,54–66].

During a sinusoidal pitching motion, the pitch rate varies harmonically which makes it harder to isolate its influence on the onset and development of dynamic stall. To isolate the influence of the pitch rate on the occurrence and development of dynamic stall, and to better analyze the post-stall performance, constant pitch rate ramp motion may also be used [55,67–71]. The dynamic stall development for constant pitch rate motions and sinusoidal pitching motions are qualitatively similar and are characterized by the same flow development stages [72]. The typical flow development within a dynamic stall lifecycle (where the flow undergoes transition from fully attached to fully

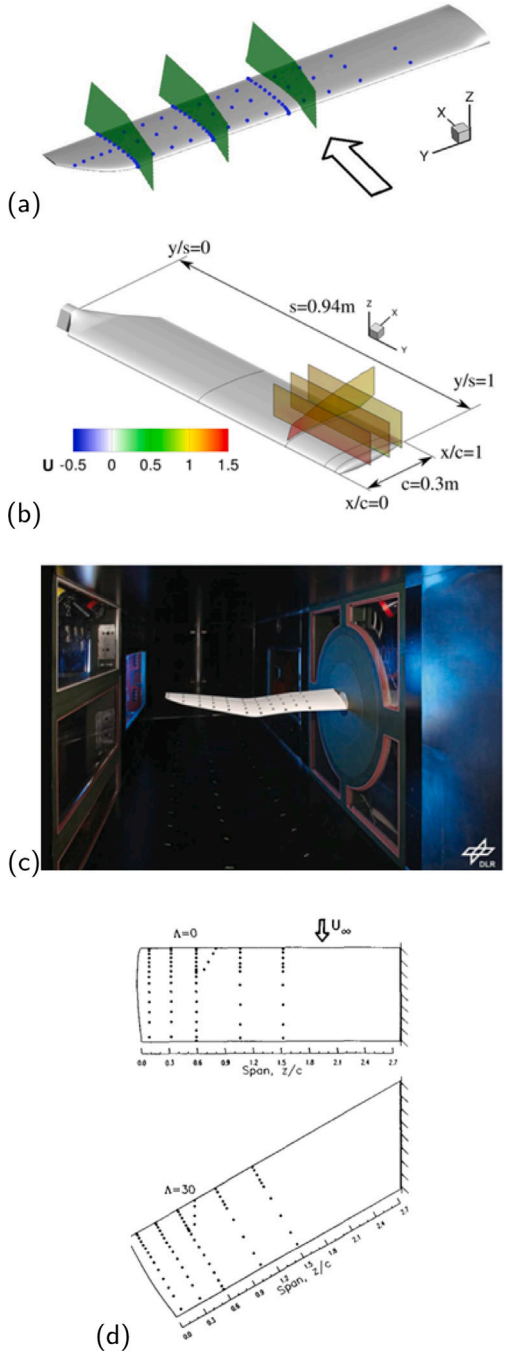

Fig. 8. Examples of finite-wing experiments. (a) Merz finite wing [44] (b) Onera finite wing [43] (c) Möwe finite wing [45] (d) UTRC swept wing [41].

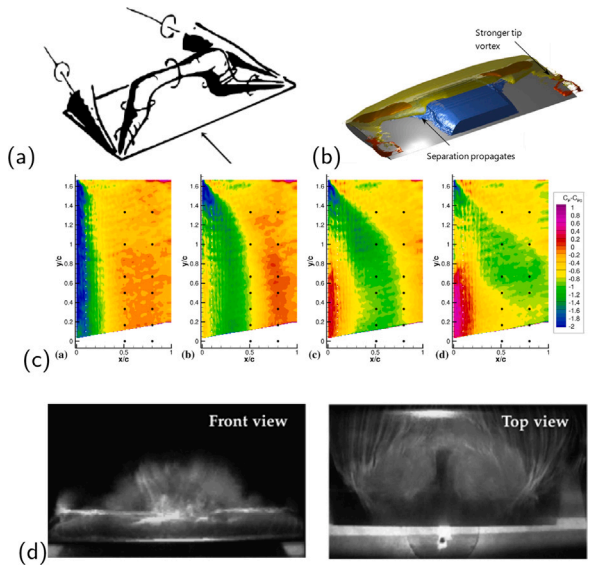

Fig. 9. Three-dimensional dynamic stall development. (a) Sketch of the Omega vortex [50] (b) Effect of aspect ratio on dynamic stall [51] (c) Three-dimensional stall vortex progression on an airfoil with PSP [52] (d) Smoke visualization of a 3D dynamic stall vortex [53].

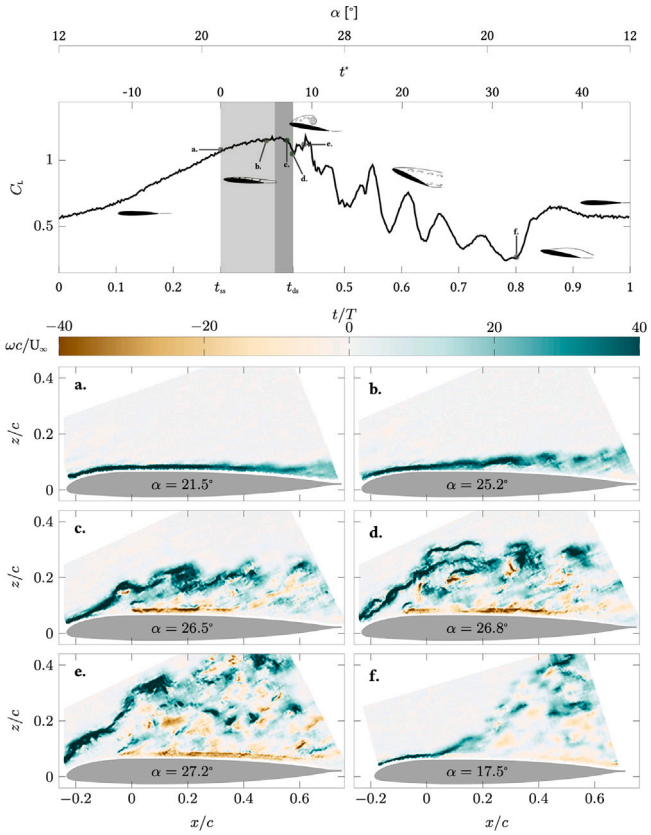

Fig. 10. Example of the typical evolution of the lift coefficient and flow during a single pitching cycle described by $\alpha = 20° \pm 8°$, $k = 0.05$ [14]. The labels a. to f. in the lift history indicate the timing of the velocity and vorticity field snapshots.

separated and back) can be divided into the following characteristic flow stages: an attached flow stage, a stall development stage, a fully stalled phase, and flow reattachment (Fig. 10). In recent work studying dynamic stall on vertical axis wind turbines or cross-flow turbines, asymmetric pitching motions or pitching motions around a zero mean angle of attack have also been evaluated, with stall observed at both positive and negative extrema [73–76].

A large number of pitching airfoil experiments have been performed for incompressible flow Mach numbers and for Reynolds numbers of the order of 10^5 and 10^6, resulting in an improved understanding of the dynamic stall process. The classic dynamic stall response under these conditions includes a delayed onset of stall (to higher angle of attack), a rapid drop in lift with large load hysteresis, and a short-duration impulsive peak in pitching moment followed by smaller secondary peaks and a negative pitching moment. The dynamic stall onset is

associated with the separation or shedding of a large scale dynamic stall vortex. At low Reynolds numbers and on thin airfoils or flat plates, the dynamic stall vortex is a classic leading-edge vortex that is fed by the leading-edge shear layer. At higher Reynolds numbers and on thicker airfoils, the dynamic stall vortex forms as a result of the roll-up of the shear layer that covers the airfoil suction surface and consists of many small scale coherent structures [77,78].

Two-dimensional airfoil experiments have significantly advanced the knowledge on the role of surface vorticity for unsteady flow separation [67,68,79], identification and prediction of the dynamic stall onset [14,80–82] and the associated stall delay [66,77,83–86], and the dominant velocity and load fluctuations [16,17,62,63,87–90]. Shih et al. [69] were among the first to highlight the importance of time-resolved flowfield measurements for the analysis of dynamic stall due to its inherent unsteady and non-periodic response. The first time-resolved particle image velocimetry (PIV) recordings of a full dynamic stall life cycle on a pitching airfoil were conducted by Mulleners and Raffel [14].

The pitching airfoil setup is affected by wind tunnel installation, including the side-wall connection [91,92], which can lead to significant differences in the measured peak pitching moment and lift coefficients relative to a two-dimensional flow [93]. Part of this is due to the transport of vorticity away from the centerline of the model because the dynamic stall vortex on this type of wing installation is typically curved rather than entirely normal to the flow direction [52] due to end effects (see also Fig. 9).

In general, stall onset on a pitching wing is delayed to higher angle of attack with increased pitch rate, but the non-dimensional stall delay (i.e., the time between passing the static stall angle and dynamic stall multiplied by v_∞/c, [14]) decreases with increased reduced pitch rate [17,69,71,86]. For sinusoidal pitching motions, the rate of change of the angle of attack at the time when the static stall angle is exceeded is identified as a single parameter that can be used to describe the overall influence of the airfoil's unsteadiness on the stall development [14,94]. This instantaneous effective unsteadiness parameter equals the reduced pitch rate for ramp-up motions.

The vast majority of experiments mentioned above have been performed at relatively low Mach numbers. The dynamic stall process at Mach numbers above 0.4 has received considerably less attention than its incompressible counterpart. For transonic Mach numbers, dynamic stall onset is related to shock-induced separation and results in a shock-buffet type stall, with circulation shedding through a small-vortex shear stream rather than a single dynamic stall vortex [95–97]. These flows are characterized by a continuously increasing pitching moment with increasing angle of attack instead of a distinct pitching moment peak as observed at subsonic Mach numbers (see Fig. 11).

Pitching airfoil tests are attractive due to the ability to instrument the model with a large number of pressure sensors to extract most features of stall and even reconstruct sectional pressure forces. Mach and Reynolds numbers relevant to helicopter main rotors can often be achieved. 3D CFD is required to capture the effects of even large aspect ratio geometries and boundary conditions. It is possible to combine results from pitching airfoil experiments and CFD to optimize airfoil dynamic stall performance [64]. Fundamental experiments remain important to achieve a better understanding of the fundamental fluid mechanics of the dynamic stall process. At lower Mach and Reynolds numbers, structural loads are reduced, and thus experiments in this regime offer higher relative stiffness and better control of the boundary conditions, thereby enabling detailed studies of the flow physics that are difficult to achieve in other types of experiments where spatial and temporal measurement resolution may be limited.

3.5. Fundamental experiments

Many investigations focusing on the underlying flow physics of dynamic stall rely on fundamental experiments. These types of experiments have often been performed at low Reynolds numbers where the time scales of flow development tend to be long enough to permit highly temporally and spatially resolved measurements, thereby enabling the detailed study of the dynamic stall vortex formation, growth, separation, convection, and wake evolution. Examples of these types of experiments shown in Fig. 12 include flow separation and vortex formation on surging airfoils for reverse flow modeling [19,98], discrete gust encounters for flat plate wings [99], and fixed- and variable-pitch rotating wings [100], similar to that in Fig. 7a, but on a smaller scale. These experiments are often characterized by the high quality of the experimental data, and in some cases a direct comparison with classical theory can be undertaken [101–103].

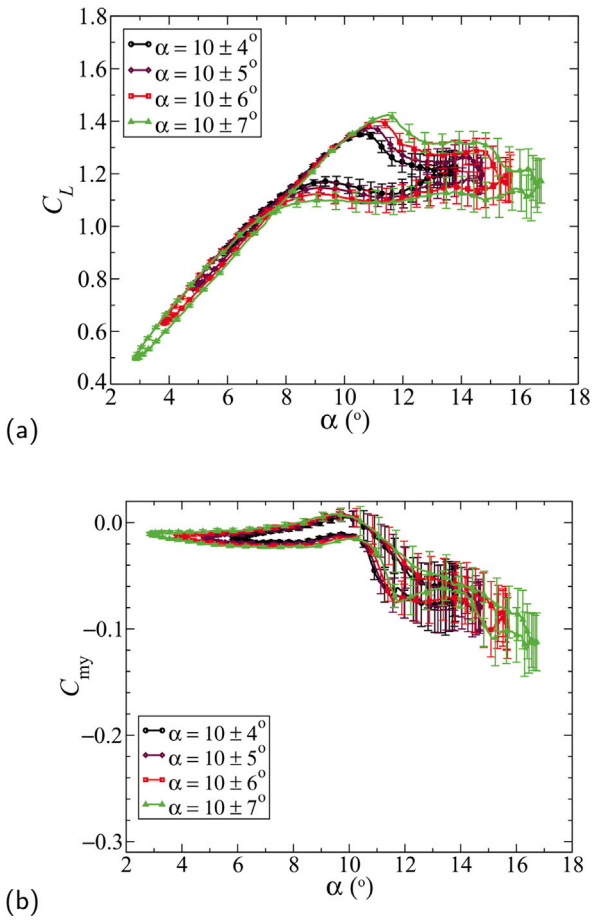

Fig. 11. Dynamic stall of the EDI-M109 airfoil at Mach 0.5, contrast Fig. 2 for the same airfoil at Mach 0.3 [15]. (a) Lift (b) Pitching moment.

Fundamental experiments have been performed over a wide range of low Reynolds numbers $\mathcal{O}(10^2–10^5)$ and for a wide variety of wing geometries and kinematics including pitching, plunging, surging, flapping, and/or rotating. Various maneuvers and accelerations have been studied for both transient and periodic motions in quiescent flow, steady flow, and unsteady flow (e.g., unsteady wind tunnels, blade-vortex interactions, and gust encounters). The most prominent experiments on maneuvering wings are summarized in Refs. [104,105] and others on gust encounters are described in Refs. [5,22,106]. Even though many of these pitching airfoil experiments use a two-dimensional wall-to-wall test model (see Section 3.4), the flow development during dynamic stall is inherently three-dimensional. To specifically investigate the effects of three-dimensionality (i.e., spanwise flow and tip vortices, respectively) studies have also been performed on swept and finite wings (see Section 3.3). In the latter case, experiments have largely been motivated by insect flight and other small-scale low-speed fliers, and have focused on rigid low aspect ratio wings.

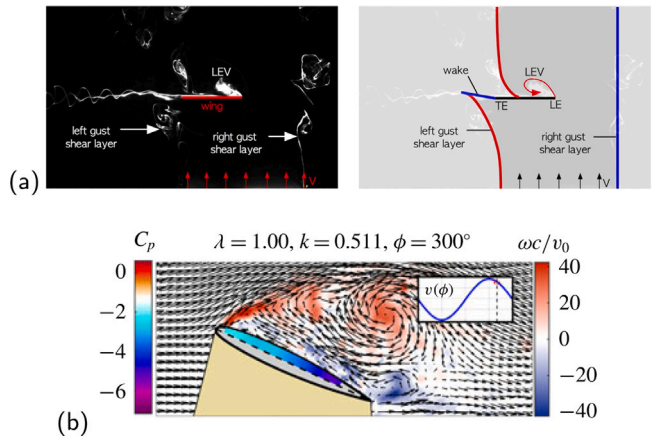

Fig. 12. Examples of fundamental experiments. (a) Gust encounter on a flat plate wing [99] (b) Surging wing oscillating into reverse flow [19].

These flows are necessarily three-dimensional and are categorized here rather than with other rotor experiments because for a rigid, low aspect ratio wing in hover, the vortex that forms as a result of flow separation at the leading edge (typically called the leading-edge vortex) remains attached to the wing for some length of time. This permits in-depth measurements of the three-dimensional vortex structure that are difficult to achieve on larger scale rotors in forward flight and represents the dynamic stall vortex before it separates from a larger scale rotor.

Even at relatively low Reynolds numbers it is possible to generate a dynamic stall or leading-edge vortex (LEV) on a rapidly pitching or accelerating wing. In general, a single coherent LEV forms near the start of an unsteady wing motion. In the absence of a stabilizing force (i.e., a mechanism for vorticity transport out of the core of the vortex), this vortex quickly grows to a peak strength and separates from the wing, severing the feeding shear layer. The vortex is then convected downstream, away from the wing, and the lift build-up that occurred during the growth of the LEV falls off as the flow eventually recovers to steady state. For cases where the wing remains at a high incidence relative to the inflow, subsequent vortices may form and shed, but are not generally considered LEVs. These may include vortices of the same or opposite sense of rotation as the primary LEV shed, or a shed wake emanating from the trailing edge. In some cases, notably on rotating wings, a conical three-dimensional vortex forms and thus a mechanism for vorticity transport exists. In this case, the LEV may not shed from the wing, but rather remain attached to the leading edge so long as the rate of vorticity generation at the leading edge is balanced by the rate of vorticity transport through the vortex core. This balance is characterized by the Rossby number ($\mathrm{Ro} = U/\Omega L$ where U is the freestream, Ω is the rotational velocity, and L is a characteristic length), a measure of the relative importance of Coriolis forces on a rotating system and sometimes taken to be equivalent to the aspect ratio of a rotating wing ($\mathrm{Ro} = U_{\mathrm{tip}}/\Omega L = \Omega R/\Omega c = R/c$). At low Rossby numbers, radial vorticity transport is sufficient to stabilize a coherent vortex, but vortex burst occurs at high Rossby numbers. Vortex burst occurs when the core of the LEV becomes unstable, and vorticity is no longer contained within a small core region of the flow. The result is a largely disorganized recirculating flow that does not have the same clear structure as a leading-edge vortex, but does retain sufficient recirculation with the potential for some amount of lift augmentation [107,108]. A more in-depth review of the physics and modeling of the leading-edge vortex can be found in [105].

A unifying theme of the fundamental experiments highlighted in this section is that these flows capture some subset of the essential physics of dynamic stall while still permitting high-resolution measurement of the unsteady airloads and/or flow field during leading-edge flow separation and the resulting evolution of a vortex-dominated flow. Experiments are typically designed to generate a flow with shed vortices that are both identifiable and quantifiable, thus experiments tend towards low Reynolds numbers, short time scales, and the absence of strong three-dimensional effects or background turbulence. This permits force decomposition into circulatory and non-circulatory components where the non-circulatory added mass term can be computed analytically [109]. However, challenges remain even in this relatively simple flow, and there is discussion within the community regarding how to reliably define and track the extent of the leading-edge vortex, how to define its shedding, strength and trajectory, and how to compute the effects of these flow structures on wing loading.

4. Special topics related to dynamic stall

4.1. The role of transition

Transition from laminar to turbulent flow can influence flow separation and the pressure distribution over airfoils and wings. This can directly influence the dynamic stall behavior observed in experiments and the findings elucidated previously. Transition can be difficult and costly to measure in experiments, and, given the relatively large scale and highly unsteady nature of rotary-wing vehicles in flight and wind turbines in the atmospheric boundary layer, many experimental efforts added trips to ensure fully turbulent flow conditions. Full-scale helicopters and wind turbines operate at Reynolds numbers in the transitional range [110,111], and particularly smaller rotors have significant laminar flow [40,112]. Although this laminar flow is important for performance prediction, and for the resistance to vortex-induced flow separation, flow separation driven by high angle of attack the boundary layer transition on the suction side reaches the leading edge well before the onset of flow separation, see [113], Fig. 15. For compressible flows, Ekaterinaris et al. identified the bursting of the laminar separation bubble at high angles of attack (near stall) can lead to the onset of leading-edge dynamic stall [114].

Airfoil experiments were performed with wings that stretch across or nearly across the wind tunnel. The seminal experiments for rotary-wing airfoils were conducted in the early 1980s and are reported in NASA TM 84245 [1]. They examined a variety of airfoils, including the NACA0012, SC-1095, Wortmann FX-098, HH-02, VR-7, and NLR-1 airfoils, which were designed for, or applied on, rotors. Hot-film and hot-wire sensors on the upper surface, along with shadowgraph flow visualization were applied to assess boundary layer transition, along with other characteristics of the dynamic stall tests. More recent tests reported in 2013 by Richter et al. [115] on another rotor airfoil (EDI-M109) included transition measurements using hot film anemometry and high speed pressure measurements. The transition location is highly time dependent during the stall event, and the location of the maximum upper surface transition moves farther aft as the oscillatory amplitude increases. The intermittent region increases with amplitude, and the maximum transition location varies linearly with amplitude. Movement of the transition location during the stall event reduces with increasing Mach number in the subsonic range, occurring at lower angles of attack at increasing Mach number. Hysteresis in transition location was noted to exceed that of lift, hypothesized to be due to viscous contributions not measurable with pressure taps. The variation was observed to be the same during both the upstroke and downstroke. Raffel et al. [116] validated their differential infrared thermography for transition with the two-dimensional NACA0012 airfoil. They reported up to 5% phase lag of transition with angle of attack.

Before moving to studies of rotating dynamic stall, researchers also studied transition on translating wings using rotary-wing airfoils. In particular, the influence of the wing tip on transition was studied so that the physics of more complex rotating blades could be distinguished from the three-dimensional effects. One of the more relevant studies

include ONERA evaluations on the OA209 wing [117] with natural transition. When combined with computational assessment [118], we can conclude that transition, similar to two-dimensional results, remains relevant on the inboard sections only to approximately the midspan locations, after which the flow is increasingly dominated by the influence of the tip vortex. Radial flow from root to tip was observed after separation.

For rotating systems, the rigid rotor test facility (RTG) rotor was evaluated in axial flow (with cyclic added for variation controls) by DLR with transition measurements using differential infrared thermography [40]. The transition hysteresis scales with increasing pitch rates and follows trends observed in the two-dimensional analysis. Raffel et al. [116] reported spanwise variations in transition with larger transition variations during dynamic stall occurring at the outboard section of the blade. The transition locations were discontinuous and significantly different during upstroke and downstroke at the three-quarter radial location.

As new techniques to measure transition continue to be developed, it is expected that a further understanding of the role of transition in fully rotational dynamic stall will be achieved in the near future.

4.2. Reverse flow dynamic stall

Reverse flow dynamic stall occurs when the (typically sharp) geometric trailing edge of the wing is ahead of the leading edge with respect to the direction of the incoming flow such that the geometric trailing edge of the wing acts as the aerodynamic leading edge. This occurs in rotating systems on the retreating side of the rotor disk when the forward flight velocity exceeds the rotational speed of the blade. (See Fig. 13.) As the advance ratio $\mu = \Omega R/U_\infty$ increases, the region of the rotor disk over which reverse flow occurs expands outboard, encompassing the entire blade at $\psi = 270°$ and $\mu = 1$. New rotor designs for high advance ratio vertical lift and certain wind-rotor scenarios in wind turbine applications can have significant regions of reverse flow. Reverse flow dynamic stall can be arguably easier to evaluate as a sharp trailing edge is likely to have a fixed separation point, avoiding the challenge of modeling transition and separation on a smoothly curving surface (i.e., the rounded leading edge).

Evidence of reverse flow dynamic stall was first observed as a low pressure wave passing over blade-mounted pressure sensors in the reverse flow region of a full-scale UH-60 A test at high advance ratios [120]; similar results were obtained through later computations [121]. Following this finding, a series of more canonical experiments were undertaken to better understand the details of these flow physics and the effect of sharp versus blunt trailing edge geometries [17,122–125]. A NACA 0012 blade section mounted in reverse flow and undergoing sinusoidal pitching in a constant freestream was found to undergo dynamic stall initiated by flow separation from the sharp aerodynamic leading edge (unlike traditional dynamic stall, where separation is delayed to high angles of attack). The resulting dynamic stall vortex was found to convect slower than one formed in forward flow. Unlike classic dynamic stall, reverse flow dynamic stall is only weakly sensitive to Reynolds number due to forced flow separation at the sharp aerodynamic leading edge. The number of shed vortical structures for a NACA 0012 blade section in reverse flow dynamic stall was found to vary with reduced frequency and pitch angle; at greater reduced frequencies, the primary dynamic stall vortex affected a greater portion of the cycle.

Hodara et al. [125] provide a comparison of experimental and numerical data on reverse flow dynamic stall and outline five stages of this process. The stages are described below and the resulting lift curve is shown in Fig. 15.

Stage 1: Attached flow regime. During this stage the flow over the airfoil is attached over much of the chord, separating near the blunt aerodynamic trailing edge. As the airfoil pitches downward, high velocities occur near the sharp leading edge resulting in an increase in suction.

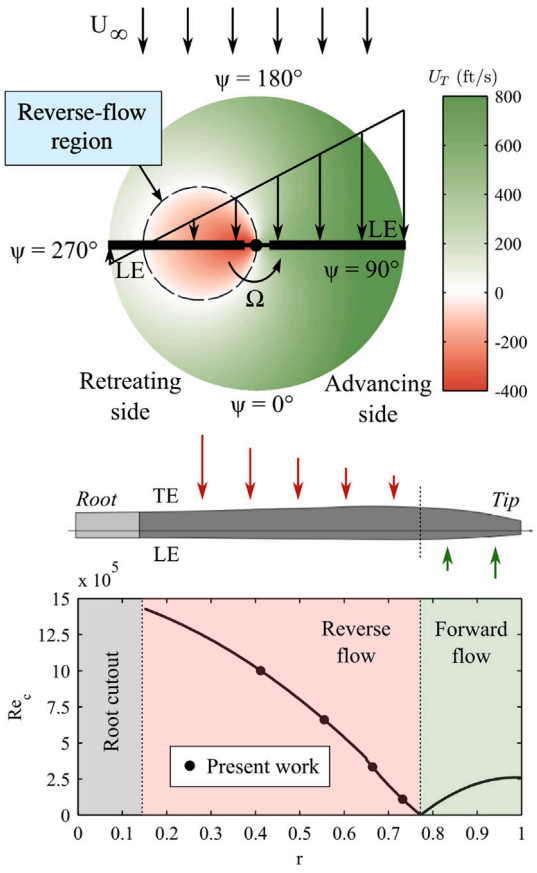

Fig. 13. Estimated velocity and Reynolds number distributions for an X2TDTM rotor $\mu = 0.77$, (250 kt) [119] (a) In-plane velocity distribution, U_T (b) Radial Reynolds-number distribution at $\psi = 270$ deg.

Stage 2: Flow separation and the formation of the primary reverse flow dynamic stall vortex. In this stage, the sharp leading edge causes the flow to separate and reattach further down the chord. The reattachment point moves downstream with increasing t/T. At some point, the flow becomes fully separated from the airfoil and the dynamic stall vortex convects downstream. The velocity of the reversed flow (i.e., flow traveling in the upstream direction) near the surface increases with the strength of the vortex.

Stage 3: Trailing edge vortex formation. The primary dynamic stall vortex induces a strong region of reversed flow in the wake that entrains the trailing-edge shear layer and leads to the formation of a trailing-edge vortex.

Stage 4: Secondary reverse flow dynamic stall vortex formation. In some cases, a secondary dynamic stall vortex forms near the sharp leading edge. The flow induced by this vortex affects a smaller region of the airfoil than the primary dynamic stall vortex.

Stage 5: Separated flow and reattachment. After the secondary vortex dissipates, the wake is characterized by turbulent separated flow. Flow begins to reattach near the leading edge, with the reattachment point moving towards the trailing edge as angle of attack decreases.

Later experiments on reverse flow dynamic stall were performed to first acquire flowfield measurements on a swept blade [62] and then moved on to perform the first flowfield measurements of reverse flow dynamic stall on a Mach-scaled rotor [18]. The rotor experiments (Fig. 14) revealed the formation and shedding of a strong vortex shed from the blunt leading edge of the blade before it enters the reverse flow region, another from the sharp leading edge of the blade in the reverse flow region (the RFDSV), and strong tip-vortex encounters at some advance ratios. Further analysis of these results focused on quantifying the three-dimensional effects of blade rotation on the reverse

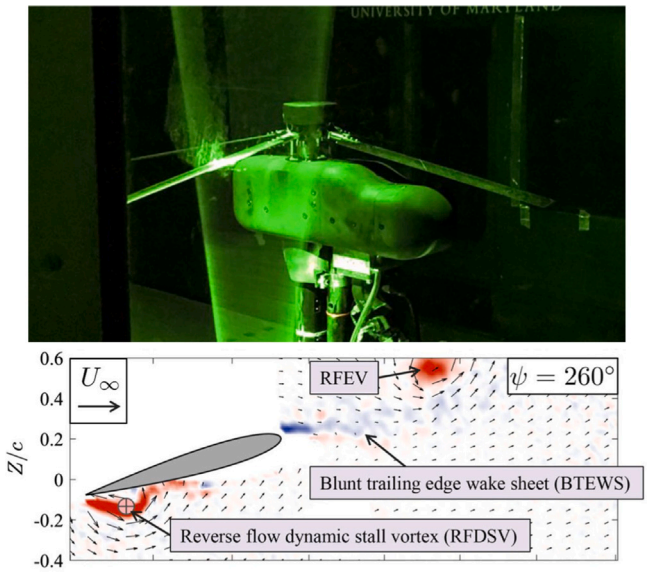

Fig. 14. Reverse flow PIV experiments in the Glenn L. Martin Wind Tunnel (GLMWT) at the University of Maryland [18] (a) Photo of the experimental rig and laser sheet installed in the GLMWT (b) Phase-averaged vorticity and flow velocity (freestream subtracted) at $\psi = 260°$ for $\mu = 0.6$.

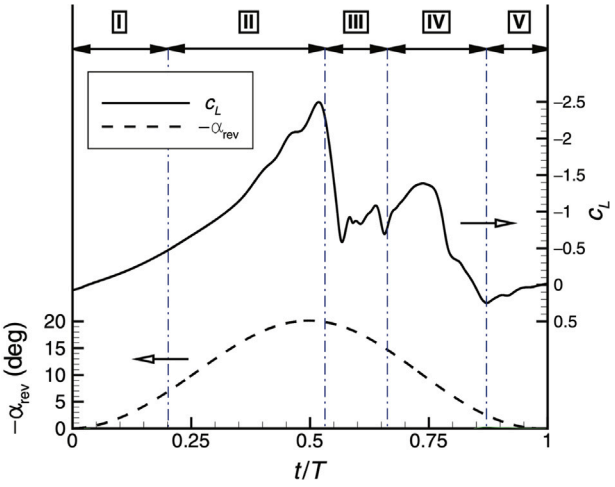

Fig. 15. Numerical predictions for the lift coefficient of a NACA 0012 airfoil in reverse dynamic stall ($Re_c = 1.65 \times 10^5$, $M = 0.1$, $\alpha_{rev} = -10° \pm 10°$, $k = 0.16$). Stages I–V of reverse flow deep dynamic stall are labeled; dash line: angle of attack; solid line: lift coefficient. From [125].

flow dynamic stall vortex [126] and on understanding the "blunt-edge" vortex that forms as the blade enters the reverse flow region [127,128].

4.3. Cycle-to-cycle fluctuations

The complexity of two-dimensional dynamic stall is evident from the discussion above. Unfortunately, an additional level of difficulty is that the dynamic stall process can vary significantly from cycle to cycle. Such variability has been demonstrated in several facilities [65,129] and is no longer characterized as an experimental uncertainty. As shown in Fig. 16, when the probability of the data scatter in (a) is plotted as a probability density function as in (b), clearly preferred paths emerge. Considering individual cycles is thus important as phase averaging disregards the complexity of the process and can suggest results that, in cases such as that shown in Fig. 16, are rarely observed. The origin of these cycle-to-cycle variations has been attributed to

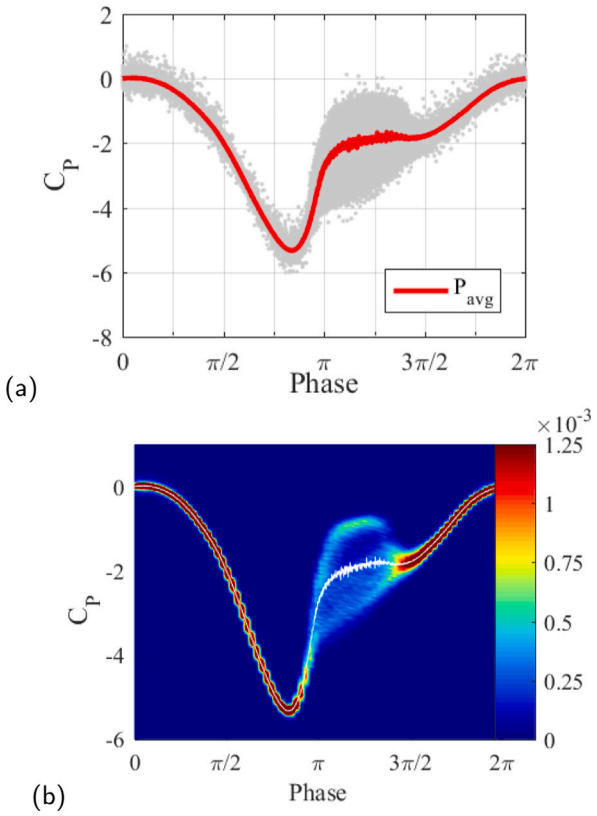

Fig. 16. Pressure coefficient on an airfoil surface at x/c =0.0225 for α= 8.5° ±9° and k = 0.01: (a) scatter plot with phase average (red) (b) joint probability density function with phase average (white) [65].

stochastic variations from turbulent boundary layer separation and shedding during full stall [14,94]. Good statistical handling of these variations is important to identify the bounds of the unsteadiness; the importance of cycle-to-cycle variation has been found to vary with airfoil and Mach number.

Cycle-to-cycle variations are not always purely stochastic. Instead, the variations are clustered into distinct groups with clear fluctuations when individual pressure locations are considered [65]. To better represent the results, groups with similar paths may be clustered together. Identifying algorithms which identify realistic, repeatable groups is ongoing, where proper orthogonal decomposition (POD)-based data clustering [64,130] and multi-dimensional scaling and clustering using dynamic time warping [131] are two promising approaches. POD clustering has been successfully used to more accurately characterize the aerodynamics of the UH-60 A wind tunnel experiment where cycle-to-cycle differences in the occurrence of stall lead to a shift in the mean values of forces relative to computational results, which, using one turbulence closure, captured only one of the multiple aerodynamic states observed in the experiment [132].

4.4. Measurement techniques and test facilities

The improvement of measurement techniques has proceeded at a rapid rate over the past decades. Surface and flow-field measurements are now available for application to dynamic stall measurement campaigns without excessive effort. An overview of many techniques relevant to dynamic stall is given in Ref. [133], from sensor-based pressure and heat flux measurements, to particle-image velocimetry (PIV) variants including micro-PIV and volumetric PIV in both the standard tomographic cross-correlation variant (Tomo-PIV) and the Lagrangian particle-tracking variant (STB). Many measurements use

Table 1
Application of measurement techniques to dynamic stall. (✓) used for dynamic stall, (×) not yet used in this situation, (•) used in other contexts.

Method	Pitching airfoil	Finite wing	Rotor in lab	Rotor in WT	Flight test
Pressure sensors	✓	✓	✓	✓	✓
Hot-film analysis	✓	✓	×	•	×
PIV (2C)	✓	✓	✓	✓	•
Micro-PIV	✓	×	×	×	×
Tomo-PIV and STB	×	×	✓	×	×
PSP/TSP	✓	×	•	•	×
BOS	✓	•	•	•	•
DIT (BL transition)	✓	✓	✓	•	•
DIT (Detect stall)	✓	×	✓	×	×

schlieren visualization, primarily in the background oriented schlieren (BOS) variant, and also interferometry, primarily before the development of BOS. Finally, surface techniques including differential infrared thermography (DIT) and luminescent paints for pressure and temperature measurement (PSP/TSP) are also reviewed. Table 1 gives an overview of typical measurement techniques.

Measurement techniques continue to be improved, leading to higher spatial and temporal resolution and new approaches for extending existing measurement techniques. The pitching airfoil was historically critical to the development of PIV for unsteady flows [134]. In recent times, the application of BOS for stall [135] has become a powerful method for analyzing the topology of the off-body flow when PIV is not possible. New analysis methods for data acquired using pressure sensors [113] and infrared cameras [136] have led to a considerable increase in the ability to study boundary layer transition in the type of unsteady flows relevant to dynamic stall, and to detect stall [133,137]. Compensation for tubing effects has allowed robust pressure scanners to be used for unsteady pressure measurements (up to 1.5 kHz for short tubes) [138,139] and has been applied to pressure measurements on oscillating airfoils [64].

In addition to the advancement of instrumentation, the modification of wind tunnel flows has been used to approach technically difficult problems. Various flows of interest include varying free-stream velocity and Mach number [140,141] and free-stream turbulence [142]. Clearly the advent of smaller and lower flight speed systems expected with unmanned air systems will need to address issues (e.g., gusts, turbulent conditions) that have smaller impacts on conventional rotorcraft [5].

In addition to improved instrumentation and facilities, the implementation of new analysis techniques for existing flow measurement techniques has resulted in an improved understanding of turbulent and separated flows through the use of statistical analysis including modal approaches (e.g., [90,143–146]), and this effort is continuing into the use of machine learning and data driven approaches (e.g., [132,147,148]). Such work promises powerful new tools for the understanding of the complex datasets now available from modern instrumentation.

Continued development of diagnostics should be a priority that goes hand in hand with the implementation of existing techniques to more challenging and relevant configurations. Techniques that work in the laboratory are often difficult to move to the more challenging flight-test environment, but yield significant benefits when successfully deployed. Increased resolution in time and space of both surface and flowfield measurements can result in new insights. Similarly, an expansion of the measurable quantities is desirable. For example, the measurement of skin friction is challenging, but can provide unique information about the state of the boundary layer [149]. The ability to measure near-wall fluctuations when surfaces are moving dynamically would allow better understanding of the onset of dynamic stall and its sensitivity to the state of the flow. Finally, smarter use of the instrumentation (e.g., sensor placement) will increase the amount of information that can be extracted.

5. Control of dynamic stall

On-blade control of flow separation and dynamic stall has been a popular research topic. One approach to dynamic stall control is to employ actuators on the main rotor blades to quickly adapt to the different flow conditions on the advancing and retreating blades. By doing so researchers would sidestep the difficulty of optimizing a single airfoil for both high-speed low-angle operation (on the advancing side of the rotor disk) and low-speed high-angle operation (on the retreating side).

Early experiments in the 1950s concentrated on increasing the maximum speed of piston-engine helicopters, which were under-powered by modern standards. They energized the boundary layer by blowing air from slots near the leading edge which significantly increased the maximum flight speed [150]. Wind tunnel investigations on this type of "boundary layer control" indicated a significant increase in maximum advance ratio before stall occurs [151]. In the decades that followed, nearly all of the gains of these early experiments have been superseded by improvements in rotor blade design. These experiments also noted several points that are still relevant today, including the similarity between effective flow control on a pitching airfoil and a rotor blade in flight. Additionally, by cyclically controlling the blowing (constant blowing only on the retreating side), the same flow control result can be obtained with only half the compressed air required by constant blowing.

There are some practical considerations that should be considered in the evaluation of dynamic stall control. For example, dynamic stall mostly occurs during transient maneuvers with wake re-ingestion and high blade elasticity. For these flight conditions, the aerodynamic angle of attack on the rotor blade is typically controllable only with an accuracy ±5° in the best case, so shifting the stall angle by 1-2° is not particularly useful. Likewise, static experiments that demonstrate a shift in the onset of stall to marginally higher angles are not particularly relevant in dynamic stall control due to the aerodynamic differences between static and dynamic stall.

Practically, control effectiveness is best measured as a reduction in the peak pitching moment as this reduces vibratory loads and pitch link loads. The associated lift control is also important, but lift hysteresis is harder to quantify, and is directly associated with a reduction in the peak pitching moment. Ideally, a dynamic stall control method should result in a significant improvement over a rotor redesign, but fixed-wing studies have shown that flow control is not likely to exceed the performance of a point-optimized airfoil [152]. Novel flow control investigation should use state-of-the art airfoil designs to obtain reliable and more relevant solutions for modern aircraft designs.

The power requirements for active flow control are an important consideration as they can be a significant fraction of the main rotor power requirements. The power requirement in experimental test cases should be scaled to evaluate the true expected power requirements for full-scale vehicles. Related to this, the difficulty of transferring power from the fuselage to the rotating blade frame must be considered when evaluating flow control measures.

Control devices can be roughly divided into three categories:

- **Flaps, slats and other camber-changing devices**, which are actuated in a 1/rev cycle. Related devices are also used for higher harmonic control with n/rev actuation and may also reduce dynamic stall by reducing blade-vortex interactions.
- **Boundary layer control** including vortex generators and other actuated or fixed devices that move energy from the outer flow into the wall-adjacent flow. These include both passive devices as well as active boundary layer control devices such as dielectric barrier discharge actuators and synthetic jets which increase the momentum of the wall-adjacent flow to delay separation.
- **Active control devices** that add a large amount of momentum to the dynamic stall vortex region to reduce the effect of dynamic stall in a fully separated flow.

The actuation of these devices can be continuous or require triggering with respect to the azimuthal position, to stall detection, or to a closed-loop control signal. The following section does not include a discussion of control devices that primarily target blade-vortex interaction and noise reduction. Since a large proportion of rotor dynamic stall in highly-loaded turning flight is caused by blade-vortex interaction, dynamic stall may be reduced or eliminated in some flight situations by these devices.

Beyond the obvious practical applications, investigating flow control measures is a useful way to gain insight into the aerodynamics of a flow phenomenon. Flow control is a path to understanding dynamic stall, and has great scientific value independent of whether it leads to a practical flow control device for a given aircraft.

5.1. Flaps and slats

Similar to wings in non-rotating flow, an active or passive alteration of airfoil camber can delay stall on a rotor blade. For example, an overview of early US Army AFDD wind tunnel results on pitching airfoils with static leading edge modifications including droop nose and slats is given by Yu et al. [153]. In this work, blowing through the slat gap was found to delay stall and reduce load hysteresis, although it also increased the negative pitching moment. Further investigation of the same leading edge slat configuration visualized the pitching airfoil flow with interferometry [154], revealing that the shear layer from the slat trailing edge moved the newly formed dynamic stall vortex further from the surface and reduced the dynamic stall loads. Similarly, Prince and Khodagolian [155] showed that airfoil ventilation using tubes leading from the pressure to the suction side of the blade could be used to suppress static stall.

A combined US Army/NASA and DLR project [57] investigated the actuated droop nose configuration for a pitching airfoil. In this experiment, the droop nose could be actuated at 1/rev, but with a phase and amplitude offset from the main pitching airfoil. A significant improvement in aerodynamic characteristics was found. In contrast with previous slat experiments where the thin structure was often found to vibrate or bend, the droop nose was found to be mechanically stiff, which provided a more consistent gap and thus angle of attack and wing load. A later project [156] investigated the structural design necessary to implement the active droop nose into a rotor and produced a prototype, but this does not appear to have been developed further.

A related control method is deformation of the airfoil via an actuated bump on the suction side which acts to increase the airfoil thickness [157] and camber. A prototype was tested on a pitching airfoil in a wind tunnel showing shift of stall to higher angles but less so than an actuated flap or droop nose of similar complexity.

Camber change by an active 1/rev trailing edge flap also delays dynamic stall. For example, Samara and Johnson [158] performed experiments on an 18.4% thickness pitching airfoil with a flap of 20% of chord covering 60% of the 584 mm model span. An optimization of the phase and duration of the flap actuation cycle can improve the effectiveness of the flow control in a manner similar to the aforementioned droop nose approach [159]. The typical camber-changing control approach increases camber near stall to encourage flow to remain attached to higher angle of attack. A related study by Gerontakos and Lee [160] showed that upward deflections of a trailing edge flap post stall could reduce the nose-down pitching moment, especially in the case of large flap deflections. Onera's Active Flaps ABS model rotor wind tunnel study [161] was later flown by Eurocopter (now Airbus Helicopter) on the blue pulse flight demonstrator [162].

One potential variant with a much smaller moving mass is the Gurney flap and its variants, named after American race car driver Dan Gurney. The vertical flap, typically 1%–5% chord and attached vertically downward at the airfoil trailing edge, was first scientifically described by Liebeck [165], though the idea dates back to the 1930s [166,167]. This miniature trailing-edge flap was extensively investigated for transonic transport aircraft with flight tests on an A340 test aircraft in the EU project AWIATOR (Aircraft WIng Advanced Technology OpeRations), with accompanying two-dimensional static airfoil wind tunnel tests [152,168]. A core problem with this approach is how to embed a flap actuation mechanism near the trailing edge where the airfoil is thin. In AWIATOR, a split-flap was actuated with spindle actuators in a semi-static manner.

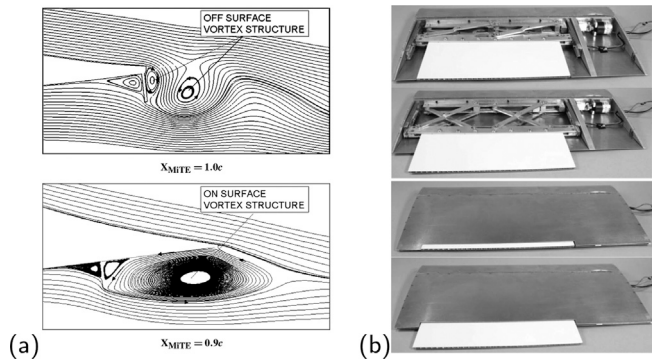

Fig. 17. Trailing edge modification of the airfoil (a) Gurney-flap variants, from [163] (b) actively actuated splitter plate, from [164].

A solution was proposed to offset the Gurney flap from the trailing edge [163] as shown in Fig. 17a, leading to the Miniature Trailing Edge effector (MiTE), which was implemented in a two-dimensional pitching airfoil. This idea was further pursued as the Active Gurney Flap (AGF) in the EU Clean Sky GRC (Green RotorCraft) program, leading to an actuated flap that could be withdrawn into the airfoil, and that provided some control of dynamic stall. The L-shaped flap offset from the trailing edge was implemented into a pitching airfoil at Politecnico di Milano [169]. Tests indicated an increase in lift during attached flow and a reduction in negative damping, but no significant reduction in the negative pitching moment. An alternative is the splitter plate, tested as both a semi-static trailing edge extension [170] and as a dynamic extension for pitching airfoils [164]. (See Fig. 17b). This approach offers a similar level of dynamic stall control and a potential alternative to actuating a small object at the trailing edge since the plate extension is along the airfoil chord line.

Another approach is that of back-flow flaps, scales, or tabs, which have generated some interest for application on both fixed- and rotating-wing dynamic stall [171–173]. These passive devices, similar to shark skin scales or hairs [172,174], activate in the presence of reverse or detached flow as illustrated in Fig. 18. They have been studied in both single and multiple actuator configurations, starting with flight tests on a Messerschmidt Me 109 in 1938 [175]. More modern investigations explicitly developed these flaps to be analogous to the pop-up feathers that exist near the leading edges of some bird wings to delay stall while landing, and implemented them for static stall control on sailplanes [176,177]. Near static stall, these devices can delay the upstream propagation of trailing edge flow separation. In dynamic stall, when the tab pops up, it acts as a barrier to the reverse flow along the airfoil surface and splits the dynamic stall vortex into smaller structures. It can also act as a vortex generator just prior to stall. Most studies of these devices did not consider rotating systems and thus focus on the effect on lift. DLR [171,178] measured the resulting pitching moment and found peak pitching moment reductions of 20%–25% in deep stall. The key is the sizing and positioning of the flap, which should influence the boundary layer flow without adding substantial drag. Another observation during operation was that if the flap is open for attached flow, it produces a rearward step and flow separation.

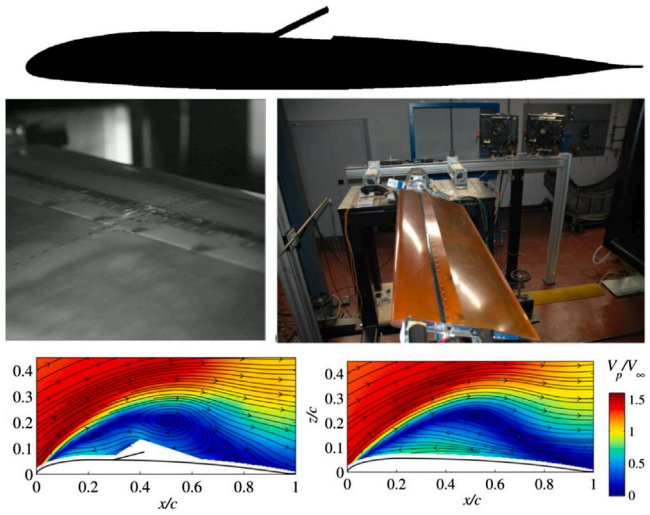

Fig. 18. Back-flow flap from [171]. Top: Idea and geometry. Center: Wind tunnel test. Bottom: PIV visualization of the method of operation (Left= Flap actuated, Right=Flap closed).

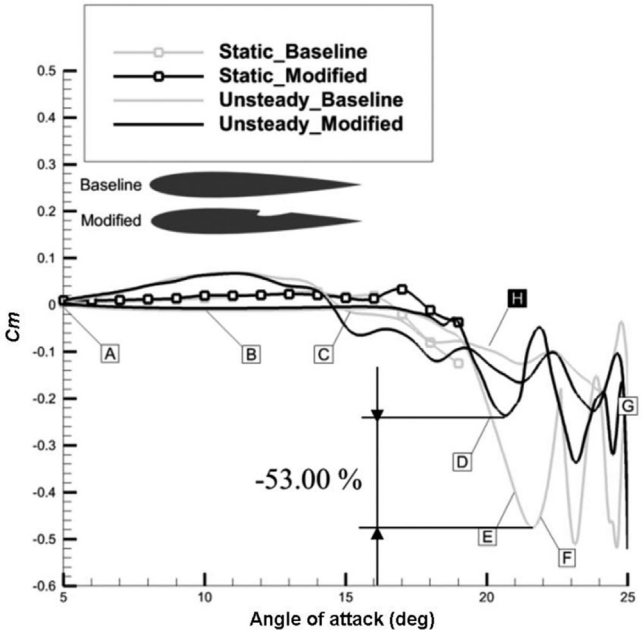

Fig. 19. Surface-based trapped vortex generators, from [185].

5.2. Boundary layer control

Another approach to dynamic stall control is to target the boundary layer and encourage higher momentum fluid from the outer flow to move into the lower momentum boundary layer, thereby providing some added measure of resistance to separation. While blade roughness can promote or increase the severity of stall [179], larger devices like vortex generators can be mounted on the blade surface to increase wall-normal convection and thereby the energy of the flow close to the wall.

An example of classic vane-type vortex generators is given by [97]. Importantly, these devices contradict the conventional philosophy that an improvement of static airfoil stall performance will also be reflected in dynamic stall. Vortex generators added to the suction side of the airfoil include a drag penalty, as shown by [180], who controlled dynamic stall using vortex generators on a pitching wind turbine airfoil.

The drag penalty of vortex generators can be reduced by changing the placement or by reducing the size of the generators. Both of these methods were implemented by the leading-edge vortex generator (LEVoG) method, which moved the vortex generators to the stagnation point for low angles of attack, thereby only "activating" them when the stagnation point moves to the underside of the airfoil at high angles of attack [181,182], reducing the drag penalty up to 5–30 counts at different flight conditions. These vortex generators have been tested for pitching airfoils where they have been shown to provide up to 25% reduction in pitching moment in deep stall, and in flight tests [183]. An alternative is to mechanically retract the vortex generators in a 1/rev phasing at parts of the cycle where they are not needed. This method was extensively studied by Onera for a co-rotating vane-type generator [60,184].

A related approach is the surface-based trapped vortex generator [185] shown in Fig. 19. Here, a deep cavity in the surface of the airfoil provides a source of large vortices that, when released, move the dynamic stall vortex further from the wall, and break it into smaller vortices, reducing the pitching moment by up to 50%, as shown in Fig. 19. The technique has some similarities with flameholders and has been shown experimentally to reduce the strength of tonal noise emitted by of thick airfoils with low oscillation amplitudes [186].

Another widely investigated actuator for active boundary layer control is the dielectric barrier discharge (DBD) plasma actuator [187–189], which has the unique advantage of being an active method of control with no moving parts. Two electrodes are separated by a dielectric barrier and driven by a high-voltage radio-frequency signal. When a high voltage is applied, the air around the actuator ionizes and results in a body force on the flow, for dynamic stall to reattach separated flows. The required momentum addition has yet to be realized experimentally.

Experimentally, DBDs have been shown to delay stall or control very light stall [190], but control authority is limited for deep stall or for flow speeds relevant to a helicopter main rotor, as shown both for NACA airfoils [191,192], and the pitching Onera OA209 airfoil [193]. One of the most successful tests of these on a pitching airfoil showed a delay of dynamic stall by about 5° at a flow speed of 15 m/s [194], with little effect at stall and at higher post-stall angles.

5.3. Active control

Active flow control is arguably the most popular concept associated with the control of dynamic stall [195]. Implementing this actuation approach requires modification of blades to include internal tubing (for blowing or suction, or steady or pulsing jets) [196], flow-through holes (for bleed or centrifugal pumping) [197], or embedded devices (e.g., synthetic jets, COMPACT jets) [198,199]. In small-scale model experiments, these approaches have shown significant reductions in pitching moment peaks, up to 80%–90% in deep stall [200]. The effectiveness of fluidic active flow control is highly dependent on the device type and the type of stall (i.e., trailing edge or leading edge), and often requires significant optimization. To date, this research has largely focused on rigid and non-rotating systems and thus the influence of rotating system dynamics and aeroelasticity remains uncertain.

Constant blowing has been demonstrated for decades to delay stall (for example, [151]), and much recent research has been motivated by a desire to achieve the same effect with lower energy requirements. Power requirements for this type of actuation at full scale can be high if internal high-pressure jets are needed, which can be an issue as many dynamic stall events occur at high thrust or during maneuvers when the additional power may not be available. Seifert et al. [201] showed that for tangential blowing from slots in the airfoil surface, pulsed blowing is more effective than constant blowing, and Nishri and Wygnanski [202] confirmed a similar effect on a generic flap. Experiments demonstrating dynamic stall control using pulsed blowing

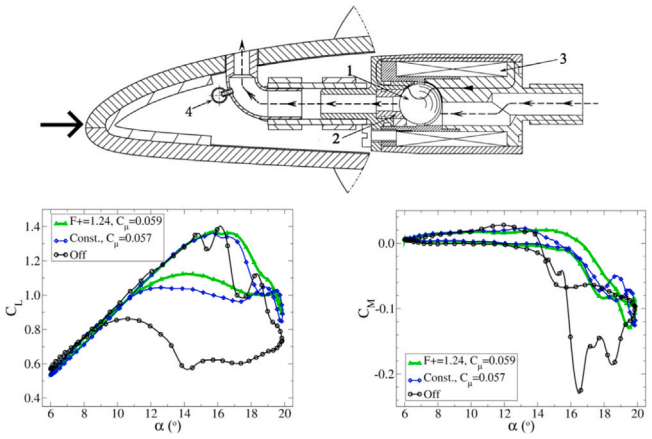

Fig. 20. Fluidic control [204]. Top: Hardware for generation of cold compressed air pulses. Bottom: Comparison of control of deep dynamic stall between pulsed and constant blowing.

from a high pressure source [200] with a normalized momentum ratio between the jets and the freestream of $0.001 \leq C_\mu \leq 0.004$, confirmed that at these blowing rates pulsed blowing was more effective than constant blowing at the same momentum ratio for weak dynamic stall. Weaver et al. [203] investigated the control of deep dynamic stall on a pitching VR7 airfoil using blowing through a tangential slot. Pulsed blowing was more effective than steady blowing for a momentum ratio $C_\mu \leq 0.01$. For the control of deep dynamic stall, a momentum ratio $C_\mu \geq 0.02$ is required and steady blowing becomes equivalent or better. DLR [96,204,205] confirmed that equivalent deep dynamic stall control requires more energy with pulsed blowing (with some limitations) than constant blowing (see Fig. 20).

The combustion-powered actuators (COMPACT) of Georgia Tech., which ignite a fuel–air mixture in chambers directly below the blade surface, offer an alternative to internal pressure jets [206], but the power required is not significantly reduced compared to compressed air, and fueling tubes must still be connected through the blade. These actuators have shown significant promise for low-speed static stall, but do not provide benefits commensurate with the power requirements for dynamic stall [199,207].

Another approach is that of bleed and synthetic jets, which require only electrical connections and tend to have lower power requirements [208]. These do still require moving parts or mechanisms. The Boeing design used by Traub et al. [209] and Nagib et al. [210] seems most successful. Power and installation requirements of active flow control devices have often impeded their implementation on rotor blades for dynamic stall, but the extensive studies to date have provided physical insights and remain a topic of interest to reduce separation and drag on fuselages and empennages [183,211].

6. Future directions and conclusion

Nearly a half-century of experimental investigations, in particular those conducted over the past decade, have yielded significant insight into the physics, prediction, and control of dynamic stall. Today, an accelerating need to better understand a broadening parameter space due to new vehicle designs and flight regimes, coupled with rapidly improving experimental capabilities and analysis techniques, motivates new types of future experiments. Some recommendations for future work are discussed below.

- The development of openly available high quality experimental databases for validation of high-fidelity computational models is critical. These should include both rigid and flexible rotors to address the expanding rotating wing designs being developed for drone, advanced air mobility (AAM), and wind turbine applications. Capturing blade deflections and flow field visualizations in the rotating frame is vital to enable validation.
- Canonical experiments targeting key flow physics and measurement quantities are necessary to focus future experiments and instrumentation development. Experiments with identical operating conditions on the same airfoil (e.g., pitching/plunging, finite fixed-wing, and rotating-wing) can separate the contributions of each effect on dynamic stall and isolate which phenomena are important at various levels of configuration complexity.
- Integration of computational studies with coordinated experimental studies are extremely valuable. The key strengths and weaknesses of the two approaches are complementary, and thus the full spectrum of underlying flow physics can be understood. Combined use of validated computational results and high-quality experimental results currently yields the greatest advancements in understanding.
- The highly unsteady flows from dynamic stall require full temporal analysis of load and pressure data. New techniques such as machine learning, artificial intelligence, complex statistics and modal representations (e.g., Ramasamy et al. [129,212,213], Taira and Nair [148]) can be used on time-resolved data to isolate and characterize the complex unsteady and aperiodic phenomena associated with dynamic stall. Further, improved test facility characterization, such as turbulent intensity across the test section inflow plane, can help to identify potential sources of unsteadiness and aperiodicity.
- Standards for experiments (e.g., number of cycles, resolution, boundary conditions, interrogation rates) should be codified and communicated to the community. Such standards can be applied to existing experiments to determine whether new, improved experiments are necessary. An expectation of high data quality should become the norm as the sophistication of applying diagnostics to these types of flows increases. Further, validation experiments should be designed collaboratively with computational experts.
- Continued development of diagnostics should be a priority. Increased resolution, lower cost and increased ease of use, measurement of quantities that are challenging today (e.g., skin friction), and smarter use of the instrumentation being used (e.g., placement) will all permit enduring use of the data acquired for validation and cost effectiveness of the experimental campaign.
- A consensus from flow control of dynamic stall is that enacting large changes in the flow requires large amounts of power. Although no on-blade active flow control method has yet been implemented on a production helicopter, flow control developments have led to improvements in stall detection, understanding of the stall process, and guidelines for airfoil development. Additional development of real-time predictions using flow sensing is also necessary to detect the onset of dynamic stall in time to avoid or mitigate it.

Advances in the understanding of dynamic stall have had a major impact in resolving the fundamental rotor performance and vibration limitations that have persisted in rotorcraft technology development. Flight envelope expansion for traditional helicopters now has considerable potential for the future. Further, the challenges related to the design of new concepts needed for Advanced Air Mobility, Unmanned Aerial Vehicles, and planetary exploration can be addressed with the surety that the limits of dynamic stall can be circumvented. New measurement techniques and improved equipment can now provide details of the flow field that were not possible to resolve a decade ago. In combination with computational efforts, it has been shown that dynamic stall on rotating systems is caused not only by the classic dynamic stall studied extensively with pitching airfoils, but also

includes separation events due to reverse flow, blade-vortex interactions, shock-airfoil interactions, and aeroelastic behaviors. Advances in experimental techniques and integration with computational efforts have already produced significantly more efficient and safer rotating wing systems for the Future Vertical Lift program in the United States and the Clean Sky program in Europe.

CRediT authorship contribution statement

Anthony D. Gardner: Writing – original draft, Reviewing and editing, Writing supervision. **Anya R. Jones:** Writing – original draft, Reviewing and editing, Writing supervision. **Karen Mulleners:** Writing – original draft, Reviewing and editing. **Jonathan W. Naughton:** Writing – original draft, Reviewing and editing. **Marilyn J. Smith:** Conceptualization, Writing – original draft, Reviewing and editing, Project supervision.

Declaration of competing interest

The authors declare the following financial interests/personal relationships which may be considered as potential competing interests: Marilyn Smith reports financial support was provided by US Army Research Laboratory.

Data availability

No data was used for the research described in the article.

Acknowledgments

The Army Research Office (ARO) workshop on dynamic stall for rotating systems at the Georgia Institute of Technology, United States was funded by Grant No. W911NF-18-1-0291. The authors would like to thank the technical monitor, Matthew Munson, for his support and guidance. This work would not be possible without the aid of many subject matter experts (SMEs) in the field of dynamic stall, who attended and/or contributed to the workshop.

K. Mulleners thanks the Swiss national science foundation (grant number PYAPP2_173652) for funding.

J. W. Naughton would like to acknowledge support under Army contract W911W60160C-0021 (Combustion Research and Flow Technology, Inc.) and subcontract SC-C-0021/C664 (University of Wyoming, United States). Further support was provided from the U.S. Department of Energy (DOE), Office of Science, Basic Energy Sciences (BES) under Award # DE-SC0001261.

A.R. Jones would like to acknowledge support under the U.S. Army/Navy/NASA Vertical Lift Research Center of Excellence Cooperative Agreement with Mahendra Bhagwat serving as Program Manager and Technical Agent, grant number W911W6-17-2-0004.

A.D. Gardner would like to acknowledge BMVg, Germany and BMWi, Germany funding under the DLR Projects FAST-Rescue and URBAN-Rescue, and BMVg funding under project 0F219.

M. J. Smith would like to acknowledge support under the U.S. Army/Navy/NASA Vertical Lift Research Center of Excellence Cooperative Agreement with Mahendra Bhagwat serving as Program Manager and Technical Agent, grant number W911W6-17-2-0004 and ARO, United States grant W911NF-13-1-0244 with technical monitor Matthew Munson.

The authors would like to thank all of the workshop participants for their insights.

The U.S. Government is authorized to reproduce and distribute reprints notwithstanding any copyright notation thereon. The views and conclusions contained in this document are those of the authors and should not be interpreted as representing the official policies, either expressed or implied, of the U.S. Government.

References

[1] W.J. McCroskey, K.W. McAlister, L.W. Carr, S.L. Pucci, An Experimental Study of Dynamic Stall on Advanced Airfoil Section. Volume 1. Summary of the Experiment, Technical Report NASA TM-842245 and USAAVRADCOM TR 82-A-8, 1982.

[2] D. Bailey, Joint Multi-Role Technology Demonstration (JMR TD) Mission Systems Architecture Demo, in: ADD 2016 Industry Day Briefing, U.S. Army Aviation and Missile Research, Development, and Engineering Center, Huntsville, Alabama, 2016.

[3] W. Johnson, A. Datta, Requirements for Next Generation Comprehensive Analysis of Rotorcraft, in: Proceedings of the American Helicopter Society Specialists Conference on Aeromechanics, San Francisco, CA, 2008.

[4] J. Letzgus, M. Keßler, E. Krämer, Simulation of Dynamic Stall on an Elastic Rotor in High-Speed Turn Flight, J. Am. Helicopter Soc. 65 (2020) http://dx.doi.org/10.4050/JAHS.65.022002.

[5] A.R. Jones, O. Cetiner, M.J. Smith, Physics and modeling of large flow disturbances: Discrete gust encounters for modern air vehicles, Annu. Rev. Fluid Mech. 54 (1) (2022) 469–493, http://dx.doi.org/10.1146/annurev-fluid-031621-085520.

[6] A.R. Jones, Gust Encounters of Rigid Wings: Taming the Parameter Space, Phys. Rev. Fluids 5 (11) (2020) http://dx.doi.org/10.1103/PhysRevFluids.5.110513.

[7] F. Richez, Analysis of Dynamic Stall Mechanisms in Helicopter Rotor Environment, J. Am. Helicopter Soc. 63 (2) (2018) 1–11, http://dx.doi.org/10.4050/JAHS.63.022006.

[8] D. Bhattacharjee, M. Hemati, B. Klose, G. Jacobs, Optimal Actuator Selection for Airfoil Separation Control, in: 2018 Flow Control Conference, Vol. 34, 2018, http://dx.doi.org/10.2514/6.2018-3692.

[9] W.J. McCroskey, R.K. Fisher, Dynamic Stall of Airfoils and Helicopter Rotors, Technical Report AGARD-R-595, 1972, pp. 2.1–2.7.

[10] A.J. Niven, R.A.M. Galbraith, D.G.F. Herring, Analysis of reattachment during ramp down tests, Vertica 13 (2) (1989) 187 196.

[11] S. Ahmed, M.S. Chandrasekhara, Reattachment studies of an oscillating airfoil dynamic stall flowfield, AIAA J. 32 (5) (1994) 1006–1012, http://dx.doi.org/10.2514/3.12087.

[12] R.B. Green, R.A.M. Galbraith, Dynamic recovery to fully attached aerofoil flow from deep stall, AIAA J. 33 (8) (1995) 1433–1440, http://dx.doi.org/10.2514/3.12565.

[13] W. Sheng, R.A.M. Galbraith, F.N. Coton, Return from Aerofoil Stall During Ramp-Down Pitching Motions, J. Aircr. 44 (6) (2007) 1856–1864, http://dx.doi.org/10.2514/1.30554.

[14] K. Mulleners, M. Raffel, The Onset of Dynamic Stall Revisited, Exp. Fluids 52 (3) (2012) 779–793, http://dx.doi.org/10.1007/s00348-011-1118-y.

[15] A.D. Gardner, K. Richter, H. Mai, A.R.M. Altmikus, A. Klein, C.H. Rohardt, Experimental Investigation of Dynamic Stall Performance for the EDI-M109 and EDI-M112 Airfoils, J. Am. Helicopter Soc. 58 (1) (2013) 1–13, http://dx.doi.org/10.4050/JAHS.58.012005.

[16] R. Gupta, P.J. Ansell, Flow Evolution and Unsteady Spectra of Dynamic Stall at Transitional Reynolds Numbers, AIAA J. 58 (8) (2020) 3272–3285, http://dx.doi.org/10.2514/1.j059040.

[17] A.H. Lind, A.R. Jones, Unsteady aerodynamics of reverse flow dynamic stall on an oscillating blade section, Phys. Fluids 28 (2016) http://dx.doi.org/10.1063/1.4958334.

[18] A.H. Lind, L.N. Trollinger, F.H. Manar, I. Chopra, A. Jones, Flowfield measurements of reverse flow on a high advance ratio rotor, Experiment. Fluids 59 (185) (2018) http://dx.doi.org/10.1007/s00348-018-2638-5.

[19] P.B. Kirk, A.R. Jones, Vortex Formation on Surging Airfoils with Application to Reverse Flow Modeling, J. Fluid Mech. 34 (859) (2018) 59–88, http://dx.doi.org/10.1017/jfm.2018.800.

[20] N. Hiremath, D. Shukla, N. Komerath, Vortical lift on retreating rotor blades at high advance ratios, Exp. Fluids 60 (6) (2019) http://dx.doi.org/10.1007/s00348-019-2740-3.

[21] L.W. Carr, M.S. Chandrasekhara, Compressibility effects on dynamic stall, Prog. Aerosp. Sci. 32 (6) (1996) 523–573, http://dx.doi.org/10.1016/0376-0421(95)00009-7.

[22] A.R. Jones, O. Cetiner, Overview of unsteady aerodynamic response of rigid wings in gust encounters, AIAA J. 59 (2) (2020) 731–736, http://dx.doi.org/10.2514/1.J059602.

[23] W.G. Bousman, Qualitative Examination of Dynamic Stall from Flight Test Data, J. Am. Helicopter Soc. 43 (4) (1998) 279–295, http://dx.doi.org/10.4050/JAHS.43.279.

[24] S. Surrey, B. Ortun, K.V. Truong, F. Wienke, Investigation of the Structural Blade Dynamics and Aeroelastic Behavior of the 7A Rotor, in: Proceedings of the American Helicopter Society 72nd Annual Forum, West Palm Beach, FL, 2016.

[25] F. Richez, R. Jain, A. Grubb, M. Smith, C. Castells, Validation and analysis of aero-elastic simulations of the UH-60A rotor from pre to post-stall flight conditions, in: Vertical Flight Society 76th Annual Forum, Virginia Beach, USA, 2020.

[26] W.G. Bousman, UH-60 Airloads Program Tutorial, in: Proceedings of the American Helicopter Society 65th Annual Forum, Grapevine, Texas, 2009.

[27] K. Mulleners, K. Kindler, M. Raffel, Dynamic Stall on a Fully Equipped Helicopter Model, Aerosp. Sci. Technol. 19 (2012) 72–76, http://dx.doi.org/10.1016/j.ast.2011.03.013.

[28] A. Bauknecht, X. Wang, J.A. Faust, I. Chopra, Wind Tunnel Test of a Rotorcraft with Lift Compounding, J. Am. Helicopter Soc. 66 (1) (2022) 1–16, http://dx.doi.org/10.4050/JAHS.66.012002.

[29] N.K. Koratkar, I. Chopra, Wind Tunnel Testing of a Mach-Scaled Rotor Model with Trailing-Edge Flaps, in: American Helicopter Society 56th Annual Forum, Virginia Beach, VA, 2000.

[30] T.R. Norman, P. Shinoda, R.L. Peterson, A. Datta, Full-Scale Wind Tunnel Test of the UH-60A Airloads Rotor, in: American Helicopter Society 67th Annual Forum Proceedings, Virginia Beach, Virginia, 2011.

[31] A. Grubb, C. Castells, R. Jain, F. Richez, M. Smith, High fidelity CFD analyses of dynamic stall on a four-bladed fully articulated rotor system, in: 74th American Helicopter Society International Annual Forum & Technology Display, Arizona, USA, 2018.

[32] M. Raffel, F. de Gregorio, K. de Groot, O. Schneider, G. Gibertini, A. Seraudie, On the Generation of a Helicopter Aerodynamic Database, Aeronaut. J. 115 (1164) (2011) 103–112, http://dx.doi.org/10.1017/S0001924000005492.

[33] P. Crozier, Recent Improvements in Rotor Testing Capabilities in the ONERA S1MA Wind Tunnel, in: Proceedings of the 20th European Rotorcraft Forum, Amsterdam, The Netherlands, 1994.

[34] X. Wang, A. Bauknecht, S. Maurya, I. Chopra, Slowed hingeless rotor wind tunnel tests and validation at high advance ratios, J. Aircr. 58 (1) (2021) 153–166, http://dx.doi.org/10.2514/1.C035900.

[35] T. Schwermer, A.D. Gardner, M. Raffel, A Novel Experiment to Understand the Dynamic Stall Phenomenon in Rotor Axial Flight, J. Am. Helicopter Soc. 64 (1) (2019) http://dx.doi.org/10.4050/JAHS.64.012004.

[36] V. Raghav, Radial flow effects on a retreating rotor blade (Ph.D. thesis), Georgia Tech, North Avenue NW, Atlanta, GA, 2014.

[37] V. Heuscheider, Parameter Identification of the MERIT Rotor Based on Hover Measurements With Collective and Cyclic Pitch Controls, in: Vertical Flight Society 78th Annual Forum, Fort Worth, Texas, 2022.

[38] S. Schreck, The NREL full-scale wind tunnel experiment introduction to the special issue, Wind Energy 5 (2–3) (2002) 77–84, http://dx.doi.org/10.1002/we.72.

[39] H. Snel, J.G. Schepers, B. Montgomerie, The MEXICO project (Model experiments in controlled conditions): The database and first results of data processing and interpretation, J. Phys. Conf. Ser. 75 (2007) 012014, http://dx.doi.org/10.1088/1742-6596/75/1/012014.

[40] A. Weiss, C.C. Wolf, K. Kaufmann, J.N. Braukmann, J.T. Heineck, M. Raffel, Unsteady Boundary-Layer Transition Measurements and Computations on a Rotating Blade Under Cyclic Pitch Conditions, Exp. Fluids 61 (61) (2020) 785–796, http://dx.doi.org/10.1007/s00348-020-2899-7.

[41] P.F. Lorber, F.O. Carta, A.F. Covino Jr., An Oscillating Three-Dimensional Wing Experiment: Compressibility, Sweep, Rate, Waveform and Geometry Effects on Unsteady Separation and Dynamic Stall, United Technologies Research Center Report R92-958325-6, 1992.

[42] R.A. Piziali, 2-D and 3-D Oscillating Wing Aerodynamics for a Range of Angles of Attack Including Stall, Technical Report NASA TM-4632, 1994.

[43] K. Kaufmann, M. Costes, F. Richez, A.D. Gardner, A. Le Pape, Numerical Investigation of Three-Dimensional Static and Dynamic Stall on a Finite Wing, J. Am. Helicopter Soc. 60 (3) (2015) 1–12, http://dx.doi.org/10.4050/JAHS.60.032004.

[44] C.B. Merz, C.C. Wolf, K. Richter, K. Kaufmann, A. Mielke, M. Raffel, Spanwise Differences in Static and Dynamic Stall on a Pitching Rotor Blade Tip Model, J. Am. Helicopter Soc. 62 (1) (2017) 785–796, http://dx.doi.org/10.4050/JAHS.62.012002.

[45] B. Lütke, J. Nuhn, Y. Govers, M. Schmidt, Design of a Rotor Blade Tip for the Investigation of Dynamic Stall in the Transonic Wind-Tunnel, Aeronaut. J. 120 (1232) (2016) 1509–1533, http://dx.doi.org/10.1017/aer.2016.74ISSN0001-9240.

[46] K. Kaufmann, C.B. Merz, A.D. Gardner, Dynamic Stall Simulations on a Pitching Finite Wing, J. Aircr. 54 (4) (2017) 1303–1316, http://dx.doi.org/10.2514/1.C034020.

[47] H. Dell'Orso, M. Amitay, Parametric Investigation of Stall Cell Formation on a NACA 0015 Airfoil, AIAA J. 56 (8) (2018) 3216–3228, http://dx.doi.org/10.2514/1.J056850.

[48] K. Kaufmann, A.D. Gardner, M. Costes, Comparison between two-dimensional and three-dimensional dynamic stall, in: New Results in Numerical and Experimental Fluid Mechanics X, in: Notes on Numerical Fluid Mechanics and Multidisciplinary Design, vol. 132, 2016, pp. 315–325, http://dx.doi.org/10.1007/978-3-319-27279-5_28, New Results in Numerical and Experimental Fluid Mechanics.

[49] A.D. Gardner, C.B. Merz, C.C. Wolf, Effect of sweep on a pitching finite wing, J. Am. Helicopter Soc. 64 (3) (2019) http://dx.doi.org/10.4050/JAHS.64.032007.

[50] F. Coton, R. Galbraith, An experimental investigation on three- dimensional dynamic stall on a finite wing, Aeronaut. J. 103 (1023) (1999) 229–236, http://dx.doi.org/10.1017/S0001924000027895.

[51] I. Andreu Angulo, P.J. Ansell, Influence of Aspect Ratio on Dynamic Stall of a Finite Wing, AIAA J. 57 (7) (2019) 2722–2733, http://dx.doi.org/10.2514/1.J057792.

[52] A.D. Gardner, C. Klein, W.E. Sachs, U. Henne, H. Mai, K. Richter, Investigation of three-dimensional dynamic stall on an airfoil using fast response pressure sensitive paint, Exp. Fluids 55 (9) (2014) 1–13, http://dx.doi.org/10.1007/s00348-014-1807-4.

[53] S. Moir, F. Coton, An Examination of the Dynamic Stalling of Two Wing Planforms, Technical Report 9526, Glasgow University, 1995.

[54] K.W. McAlister, S.L. Pucci, W.J. McCroskey, L.W. Carr, An Experimental Study of Dynamic Stall on Advanced Airfoil Sections Volume II Pressure and Force Data, Technical Report TR-82-A-8, NASA, 1982.

[55] R.B. Green, M. Giuni, Dynamic Stall Database R and D 1570-AM-01: Final Report, Technical Report, University of Glasgow, 2017, http://dx.doi.org/10.5525/gla.researchdata.464.

[56] A.J. Niven, R.A.M. Galbraith, Modelling dynamic stall vortex inception at low Mach numbers, Aeronaut. J. 101 (1002) (1997) 67–76, http://dx.doi.org/10.1017/S0001924000066732.

[57] P.B. Martin, K.W. McAlister, M.S. Chandrasekhara, W. Geissler, Dynamic Stall Measurements and Computations for a VR-12 Airfoil with a Variable Droop Leading Edge, in: American Helicopter Society 59th Annual Forum, Phoenix, Arizona, 2003.

[58] W. Geißler, G. Dietz, H. Mai, J. Bosbach, H. Richard, Dynamic stall and its passive control investigations on the OA209 airfoil section, in: 31st European Rotorcraft Forum, Florence, Italy, 2005.

[59] A. Zanotti, G. Gibertini, Experimental investigation of the dynamic stall phenomenon on a NACA 23012 oscillating airfoil, Proc. Inst. Mech. Eng. G 227 (9) (2012) 1375–1388, http://dx.doi.org/10.1177/0954410012454100.

[60] G. Joubert, A. Le Pape, B. Heine, S. Huberson, Deployable vortex generator dynamic stall alleviation through experimental and numerical investigations, J. Am. Helicopter Soc. 58 (3) (2013) http://dx.doi.org/10.4050/JAHS.58.032005.

[61] H.F. Müller-Vahl, C. Strangfeld, C.N. Nayeri, C.O. Paschereit, D. Greenblatt, Control of thick airfoil, deep dynamic stall using steady blowing, AIAA J. 53 (2) (2015) 277–295, http://dx.doi.org/10.2514/1.J053090.

[62] L.R. Smith, A.R. Jones, Measurements on a yawed rotor blade pitching in reverse flow, Phys. Rev. Fluids 4 (034703) (2019) http://dx.doi.org/10.1103/PhysRevFluids.4.034703.

[63] J. Hodara, A. Lind, A. Jones, M.J. Smith, Collaborative Investigation of the Aerodynamic Behavior of Airfoils in Reverse Flow, in: American Helicopter Society 71st Annual Forum, Virginia Beach, VA, 2015.

[64] P. Nikoueeyan, T. Harms, J. Naughton, V. Ahuja, Experimental assessment of an airfoil optimized to delay the onset of dynamic stall, in: Proceedings of the Vertical Flight Society 75th Annual Forum, Philadelphia, Pennsylvania, 2019.

[65] T. Harms, P. Nikoueeyan, J.W. Naughton, An experimental evaluation of cycle-to-cycle variations of dynamic stall, in: AIAA–2018–1267, AIAA SciTech Forum, 2018, http://dx.doi.org/10.2514/6.2018-1267.

[66] G. He, J. Deparday, L. Siegel, A. Henning, K. Mulleners, Stall Delay and Leading-Edge Suction for a Pitching Airfoil with Trailing-Edge Flap, AIAA J. 58 (12) (2020) 5146–5155, http://dx.doi.org/10.2514/1.j059719.

[67] P.F. Lorber, F.O. Carta, Airfoil dynamic stall at constant pitch rate and high Reynolds number, J. Aircr. 25 (6) (1988) 548–556, http://dx.doi.org/10.2514/3.45621.

[68] M. Acharya, M.H. Metwally, Unsteady pressure field and vorticity production over a pitching airfoil, AIAA J. 30 (2) (1992) 403–411, http://dx.doi.org/10.2514/3.10931.

[69] C. Shih, L. Lourenco, L.V. Dommelen, A. Krothapalli, Unsteady flow past an airfoil pitching at a constant rate, AIAA J. 30 (5) (1992) 1153–1161, http://dx.doi.org/10.2514/3.11045.

[70] R. Gupta, P.J. Ansell, Unsteady Flow Physics of Airfoil Dynamic Stall, AIAA J. 57 (1) (2018) 165–175, http://dx.doi.org/10.2514/1.j057257.

[71] J. Kiefer, C.E. Brunner, M.O.L. Hansen, M. Hultmark, Dynamic stall at high Reynolds numbers induced by ramp-type pitching motions, J. Fluid Mech. 938 (2022) A10, http://dx.doi.org/10.1017/jfm.2022.70.

[72] W.J. McCroskey, The Phenomenon of Dynamic Stall, Technical Report NASA TM-81264, 1981.

[73] R. Dunne, B.J. McKeon, Dynamic stall on a pitching and surging airfoil, Exp. Fluids 56 (8) (2015) 157, http://dx.doi.org/10.1007/s00348-015-2028-1.

[74] C.E. Brunner, J. Kiefer, M.O.L. Hansen, M. Hultmark, Unsteady effects on a pitching airfoil at conditions relevant for large vertical axis wind turbines, J. Phys. Conf. Ser. 1618 (5) (2020) 052065, http://dx.doi.org/10.1088/1742-6596/1618/5/052065.

[75] S. Henne, S.L. Fouest, K. Mulleners, Dynamic stall on an airfoil undergoing VAWT blade angle of attack variations, J. Phys. Conf. Ser. 1618 (2020) 052033, http://dx.doi.org/10.1088/1742-6596/1618/5/052033.

[76] S. Otomo, S. Henne, K. Mulleners, K. Ramesh, I.M. Viola, Unsteady lift on a high-amplitude pitching aerofoil, Exp. Fluids 62 (6) (2021) 1–18, http://dx.doi.org/10.1007/s00348-020-03095-2.

[77] J. Deparday, K. Mulleners, Modeling the interplay between the shear layer and leading edge suction during dynamic stall, Phys. Fluids 31 (10) (2019) 107104, http://dx.doi.org/10.1063/1.5121312.

[78] R. Miotto, W. Wolf, D. Gaitonde, M. Visbal, Analysis of the onset and evolution of a dynamic stall vortex on a periodic plunging aerofoil, J. Fluid Mech. 938 (2022) A24, http://dx.doi.org/10.1017/jfm.2022.165.

[79] M. Melius, K. Mulleners, R. Bayoán Cal, The role of surface vorticity during unsteady separation, Phys. Fluids 30 (045108) (2018) http://dx.doi.org/10.1063/1.5006527.

[80] W. Sheng, R.A.M. Galbraith, F.N. Coton, A New Stall-Onset Criterion for Low Speed Dynamic-Stall, J. Sol. Energy Eng. 128 (4) (2005) 461–471.

[81] W. Sheng, R.A.M. Galbraith, F.N. Coton, Prediction of Dynamic Stall Onset for Oscillatory Low-Speed Airfoils, J. Fluids Eng. 130 (10) (2008) http://dx.doi.org/10.1115/1.2969450, 101204 8.

[82] X. Li, L.H. Feng, Critical indicators of dynamic stall vortex, J. Fluid Mech. 937 (2022) A16, http://dx.doi.org/10.1017/jfm.2022.30.

[83] K. Mulleners, M. Raffel, Dynamic stall development, Exp. Fluids 54 (2) (2013) http://dx.doi.org/10.1007/s00348-013-1469-7.

[84] C. Fagley, J. Seidel, T. McLaughlin, Cyber-Physical Flexible Wing for Aeroelastic Investigations of Stall and Classical Flutter, J. Fluids Struct. 67 (2016) 34–47, http://dx.doi.org/10.1016/j.jfluidstructs.2016.07.021.

[85] E. Culler, C. Fagley, J. Seidel, T. McLaughlin, J. Farnsworth, Developing a reduced order model from structural kinematic measurements of a flexible finite span wing in stall flutter, J. Fluids Struct. 71 (2017) 56–69, http://dx.doi.org/10.1016/j.jfluidstructs.2017.03.010.

[86] S.L. Fouest, J. Deparday, K. Mulleners, The dynamics and timescales of static stall, J. Fluids Struct. 104 (103304) (2021) 1–11, http://dx.doi.org/10.1016/j.jfluidstructs.2021.103304.

[87] B.J. Pruski, R.D.W. Bowersox, Leading-Edge Flow Structure of a Dynamically Pitching NACA 0012 Airfoil, AIAA J. 51 (5) (2013) 1042 1053, http://dx.doi.org/10.2514/1.j051673.

[88] P.O. Bowles, T.C. Corke, D.G. Coleman, F.O. Thomas, M. Wasikowski, Improved Understanding of Aerodynamic Damping through the Hilbert Transform, AIAA J. 52 (11) (2014) 2384–2394, http://dx.doi.org/10.2514/1.J052630.

[89] E. Culler, J. Farnsworth, Higher frequencies in stall flutter moment development, J. Fluids Struct. 85 (2019) 181–198, http://dx.doi.org/10.1016/j.jfluidstructs.2019.01.007.

[90] P.J. Ansell, K. Mulleners, Multiscale Vortex Characteristics of Dynamic Stall from Empirical Mode Decomposition, AIAA J. 58 (2) (2020) 600–617, http://dx.doi.org/10.2514/1.J057800.

[91] A.D. Gardner, K. Richter, Effect of the Model-Sidewall Connection for a Dynamic Stall Airfoil Experiment, J. Aircr. 57 (1) (2020) http://dx.doi.org/10.2514/1.C035613.

[92] M.R. Visbal, D.J. Garmann, Investigation of Spanwise End Effects on Dynamic Stall of a Pitching Wing Section, J. Aircr. 56 (6) (2019) 2118–2130, http://dx.doi.org/10.2514/1.C035427.

[93] C.A. Klein, Consideration of Unsteady Effects in Helicopter Airfoil Design (Ph.D. thesis), University of Stuttgart, Stuttgart, Germany, 2016, (in German).

[94] F. Ayancik, K. Mulleners, All you need is time to generalise the Goman–Khrabrov dynamic stall model, J. Fluid Mech. R8 (2022) http://dx.doi.org/10.1017/jfm.2022.381.

[95] K. Al-Jaburi, D. Feszty, Passive flow control of shock-induced dynamic stall via surface-based trapped vortex generators, Proc. Inst. Mech. Eng. G 5 (2021) http://dx.doi.org/10.1177/09544100211011281.

[96] A.D. Gardner, K. Richter, H. Mai, D. Neuhaus, Experimental investigation of air jets to control shock-induced dynamic stall, J. Am. Helicopter Soc. 59 (2) (2014) http://dx.doi.org/10.4050/JAHS.59.022003.

[97] P. Martin, J. Wilson, J. Berry, T.-C. Wong, M. Moulton, M. McVeigh, Passive Control of Compressible Dynamic Stall, in: AIAA–2008–7506, 26th AIAA Applied Aerodynamics Conference, Honolulu, Hawaii, 2008, http://dx.doi.org/10.2514/6.2008-7506.

[98] L. Smith, A.R. Jones, Vortex Formation on a Pitching Aerofoil at High Surging Amplitudes, J. Fluid Mech. 905 (A22) (2020) http://dx.doi.org/10.1017/jfm.2020.741.

[99] S.J. Corkery, H. Babinsky, J.K. Harvey, On the development and early observations from a towing tank-based transverse wing-gust encounter test rig, Exp. Fluids 59 (135) (2018) http://dx.doi.org/10.1007/s00348-018-2586-0.

[100] Z.R. Carr, A.C. DeVoria, M.J. Ringuette, Aspect-ratio effects on rotating wings: circulation and forces, J. Fluid Mech. 767 (2015) 497–525, http://dx.doi.org/10.1017/jfm.2015.44.

[101] P. Gehlert, H. Babinsky, Linking the Unsteady Force Generation to Vorticity for a Translating and Rotating Cylinder, in: AIAA–2019–0347, AIAA Scitech 2019 Forum, San Diego, California, 2019, http://dx.doi.org/10.2514/6.2019-0347.

[102] H. Biler, C. Badrya, A.R. Jones, Experimental and Computational Investigation of Transverse Gust Encounters, AIAA J. 57 (11) (2019) 4608–4622, http://dx.doi.org/10.2514/1.J057646.

[103] I. Andreu-Angulo, H. Babinsky, H. Biler, G. Sedky, A.R. Jones, Effect of Transverse Gust Velocity Profiles, AIAA J. 58 (12) (2020) http://dx.doi.org/10.2514/1.J059665.

[104] M. Ol, H. Babinsky, Chairs, Extensions of Fundamental Flow Physics to Practical MAV Aerodynamics, NATO STO Technical Report, NATO STO, 2016, http://dx.doi.org/10.14339/STO-TR-AVT-202.

[105] J.D. Eldredge, A.R. Jones, Leading-edge vortices: Mechanics and modeling, Annu. Rev. Fluid Mech. 51 (1) (2019) 75–104, http://dx.doi.org/10.1146/annurev-fluid-010518-040334.

[106] O. Cetiner-Yildirim, A. Jones, Chairs, Unsteady Aerodynamic Response of Rigid Wings in Gust Encounters, NATO STO Technical Report STO-AVT-282, NATO STO, 2020, http://dx.doi.org/10.14339/STO-TR-AVT-282.

[107] A.R. Jones, A. Medina, H.R. Spooner, K. Mulleners, Characterizing a burst leading-edge vortex on a rotating flat plate wing, Exp. Fluids 57 (52) (2016) http://dx.doi.org/10.1007/s00348-016-2143-7.

[108] A. Medina, A.R. Jones, Leading-edge vortex burst on a low-aspect-ratio rotating flat plate, Phys. Rev. Fluids 1 (4) (2016) 044501, http://dx.doi.org/10.1103/physrevfluids.1.044501.

[109] S.J. Corkery, H. Babinsky, W.R. Graham, Quantification of added-mass effects using particle image velocimetry data for a translating and rotating flat plate, J. Fluid Mech. 870 (2019) 492–518, http://dx.doi.org/10.1017/jfm.2019.231.

[110] K. Richter, E. Schülein, B. Ewers, J. Raddatz, A. Klein, Boundary Layer Transition Characteristics of a Full-Scale Helicopter Rotor in Hover, in: Proceedings of the 72nd Annual Forum, The Vertical Flight Society, West Palm Beach, 2016.

[111] A.D. Gardner, C.C. Wolf, J.T. Heineck, M. Barnett, M. Raffel, Helicopter rotor boundary layer transition measurement in forward flight using an infrared camera, J. Am. Helicopter Soc. 65 (2020) http://dx.doi.org/10.4050/JAHS.65.012002.

[112] A.D. Gardner, A. Weiss, J.T. Heineck, A.D. Overmeyer, H.R. Spooner, R.K. Jain, C.C. Wolf, M. Raffel, Boundary Layer Transition Measured by DIT on the PSP Rotor in Forward Flight, J. Am. Helicopter Soc. 66 (2021) http://dx.doi.org/10.4050/JAHS.66.022008.

[113] A.D. Gardner, K. Richter, Boundary layer transition determination for periodic and static flows using phase-averaged pressure data, Exp. Fluids 56 (6) (2015) http://dx.doi.org/10.1007/s00348-015-1992-9.

[114] J.A. Ekaterinaris, M.S. Chandrasekhara, M.F. Platzer, Recent Developments in Dynamic Stall Measurements, Computations and Control, Reno, NV, AIAA–2005–1296, 43rd Aerospace Sciences Meeting and Exhibit, 2005, http://dx.doi.org/10.2514/6.2005-1296.

[115] K. Richter, S. Koch, A.D. Gardner, Influence of oscillation amplitude and Mach number on the unsteady transition on a pitching rotor blade airfoil, in: Proceedings of the American Helicopter Society 69th Annual Forum, Phoenix, Arizona, 2013.

[116] M. Raffel, C.B. Merz, T. Schwermer, K. Richter, Differential infrared thermography for boundary layer transition detection on pitching rotor blade models, Exp. Fluids 56 (30) (2015) http://dx.doi.org/10.1007/s00348-015-1905-y.

[117] A. Le Pape, G. Pailhas, F. David, J.-M. Deluc, Extensive wind tunnel measurements of dynamic stall phenomenon for the OA209 airfoil including 3D effects, in: 33rd European Rotorcraft Forum, Kazan, Russia, 2007.

[118] R. Jain, A. Le Pape, A. Grubb, M. Costes, F. Richez, M.J. Smith, High-resolution CFD Predictions for the Static and Dynamic Stall of a Finite-span OA209 Wing, J. Fluids Struct. 78 (2018) http://dx.doi.org/10.1016/j.jfluidstructs.2017.12.012.

[119] A.H. Lind, L.R. Smith, J.I. Milluzzo, A.R. Jones, Reynolds number effects on rotor blade sections in reverse flow, J. Aircr. 53 (5) (2016) 1248–1260, http://dx.doi.org/10.2514/1.C033556.

[120] A. Datta, H. Yeo, T.R. Norman, Experimental Investigation and Fundamental Understanding of a Full-Scale Slowed Rotor at High Advance Ratios, J. Am. Helicopter Soc. 58 (2) (2013) 1–17, http://dx.doi.org/10.4050/JAHS.58.022004.

[121] M. Potsdam, A. Datta, B. Jayaraman, Computational Investigation and Fundamental Understanding of a Slowed UH-60A Rotor at High Advance Ratios, J. Am. Helicopter Soc. 61 (2) (2016) 1–17, http://dx.doi.org/10.4050/JAHS.61.022002.

[122] A.H. Lind, J.N. Lefebvre, A.R. Jones, Time-Averaged Aerodynamics of Sharp and Blunt Trailing Edge Static Airfoils in Reverse Flow, AIAA J. 52 (2014) 2751–2764, http://dx.doi.org/10.2514/1.J052967.

[123] A.H. Lind, A.R. Jones, Vortex Shedding from Airfoils in Reverse Flow, AIAA J. 53 (9) (2015) 2621–2633, http://dx.doi.org/10.2514/1.J053764.

[124] A.H. Lind, A.R. Jones, Unsteady airloads on static airfoils through high angles of attack and in reverse flow, J. Fluids Struct. 63 (2016) 259–279, http://dx.doi.org/10.1016/j.jfluidstructs.2016.03.005.

[125] J. Hodara, A. Lind, A. Jones, M.J. Smith, Collaborative Investigation of the Aerodynamic Behavior of Airfoils in Reverse Flow, J. Am. Helicopter Soc. 61 (2) (2016) 032001, http://dx.doi.org/10.4050/JAHS.61.032001.

[126] L.R. Smith, Y.S. Jung, J.D. Baeder, A.R. Jones, The role of rotary motion on vortices in reverse flow, J. Fluid Mech. 880 (2019) 723–742, http://dx.doi.org/10.1017/jfm.2019.728.

[127] L. Smith, A.R. Jones, Unsteady Vortex Formation on Airfoils with High Surging and Pitching Amplitudes, in: AIAA–2020–1556, AIAA SciTech 2020, Orlando, FL, 2020, http://dx.doi.org/10.2514/6.2020-1556.

[128] L.R. Smith, A.R. Jones, Vortex formation on a pitching aerofoil at high surging amplitudes, J. Fluid Mech. 905 (2020) A22, http://dx.doi.org/10.1017/jfm.2020.741.

[129] M. Ramasamy, J.S. Wilson, W.J. McCroskey, P.B. Martin, Measured characteristics of cycle-to-cycle variations in dynamic stall, in: AHS Technical Meeting on Aeromechanics Design for Vertical Lift, San Francisco, CA, 2016.

[130] M. Ramasamy, A. Sanayri, J.S. Wilson, P.B. Martin, T. Harms, P. Nikoueeyan, J. Naughton, Data-driven optimal basis clustering to characterize cycle-to-cycle variations in dynamic stall measurements, in: Presented at AHS Forum 75, Philadelphia, PA, 2019.

[131] M. Lennie, J. Steenbuck, B.R. Noack, C.O. Paschereit, Cartographing dynamic stall with machine learning, Wind Energy Sci. 5 (2020) http://dx.doi.org/10.5194/wes-5-819-2020.

[132] M. Ramasamy, A. Sanayei, J.S. Wilson, P.B. Martin, T. Harms, P. Nikoueeyan, J. Naughton, Reducing uncertainty in dynamic stall measurements through data-driven clustering of cycle-to-cycle variations, J. Am. Helicopter Soc. 66 (1) (2021) 1–17, http://dx.doi.org/10.4050/JAHS.66.012003.

[133] A.D. Gardner, C.C. Wolf, M. Raffel, Review of measurement techniques for unsteady helicopter rotor flows, Prog. Aerosp. Sci. 111 (2019) http://dx.doi.org/10.1016/j.paerosci.2019.100566.

[134] M. Raffel, J. Kompenhans, P. Wernert, Investigation of the unsteady flow velocity field above an airfoil pitching under deep dynamic stall conditions, Exp. Fluids 19 (1995) 103–111, http://dx.doi.org/10.1007/BF00193856.

[135] S.C. Naigle, Flow Control of Compressible Dynamic Stall using Vortex Generator Jets (Ph.D. thesis), Ohio State University, 2016.

[136] A.D. Gardner, C. Eder, C.C. Wolf, M. Raffel, Analysis of differential infrared thermography for boundary layer transition detection, Exp. Fluids 58 (9) (2017) http://dx.doi.org/10.1007/s00348-017-2405-z.

[137] A.D. Gardner, C.C. Wolf, M. Raffel, A new method of dynamic and static stall detection using infrared thermography, Exp. Fluids 57 (9) (2016) http://dx.doi.org/10.1007/s00348-016-2235-4.

[138] J.A. Strike, M.D. Hind, M.S. Saini, J.W. Naughton, M.D. Wilson, S.A. Whitmore, Unsteady surface pressure reconstruction on an oscillating airfoil using the Wiener deconvolution method, in: AIAA–2010–4799, 27th AIAA Aerodynamic Measurement Technology and Ground Testing Conference, Chicago, Il, in: AIAA Paper 2010-4799, 2010, http://dx.doi.org/10.2514/6.2010-4799.

[139] P. Nikoueeyan, M. Hind, J. Strike, M. Singh, J. Naughton, S. Keeter, M. Dahland, Characterization of unsteady pressures on a blunt trailing edge using a direct-mount pressure scanner, in: AIAA–2019–1827, AIAA Scitech Forum, Jan 2019, 2019, http://dx.doi.org/10.2514/6.2019-1827.

[140] K. Gompertz, P. Kumar, C.D. Jensen, D. Peng, J. Gregory, J. Bons, Modification of a Transonic Blowdown Wind Tunnel to Produce Oscillating Freestream Mach Number, AIAA J. 49 (11) (2011) 2555–2563, http://dx.doi.org/10.2514/1.J051090.

[141] J. Farnsworth, D. Sinner, D. Gloutak, L. Droste, D. Bateman, Design and qualification of an unsteady low-speed wind tunnel with an upstream louver system, Exp. Fluids 61 (8) (2020) 181, http://dx.doi.org/10.1007/s00348-020-03018-1.

[142] R.J. Hearst, P. Lavoie, The effect of active grid initial conditions on high Reynolds number turbulence, Exp. Fluids 56 (2015) http://dx.doi.org/10.1007/s00348-015-2052-1.

[143] T. Harms, P. Nikoueeyan, J. Naughton, Modal analysis of the cycle-to-cycle variations observed in dynamic stall, in: Presented at AHS Forum 74, Phoenix, Az, 2018.

[144] S. Mariappan, A.D. Gardner, K. Richter, M. Raffel, Analysis of Dynamic Stall Using Dynamic Mode Decomposition Technique, AIAA J. 52 (11) (2014) 2427–2439, http://dx.doi.org/10.2514/1.J052858.

[145] D.G. Coleman, F.O. Thomas, S. Gordeyev, T.C. Corke, Parametric Modal Decomposition of Dynamic Stall, AIAA J. 57 (1) (2019) 176–190, http://dx.doi.org/10.2514/1.J057077.

[146] K.J. Asztalos, S.T.M. Dawson, D.R. Williams, Modeling the Flow State Sensitivity of Actuation Response on a Stalled Airfoil, AIAA J. 59 (8) (2021) 2901–2915, http://dx.doi.org/10.2514/1.j060304.

[147] J. Kou, W. Zhang, Data-driven modeling for unsteady aerodynamics and aeroelasticity, Prog. Aerosp. Sci. 125 (2021) 100725, http://dx.doi.org/10.1016/j.paerosci.2021.100725.

[148] K. Taira, A.G. Nair, Network-based analysis of fluid flows: Progress and outlook, Prog. Aerosp. Sci. 131 (2022) 100823, http://dx.doi.org/10.1016/j.paerosci.2022.100823.

[149] J.W. Naughton, M. Sheplak, Modern developments in shear stress measurement, Prog. Aerosp. Sci. 38 (2002) 515–570, http://dx.doi.org/10.1016/s0376-0421(02)00031-3.

[150] S.H. Hinton, Application of boundary layer control to rotor blades, J. Am. Helicopter Soc. 2 (2) (1957) http://dx.doi.org/10.4050/JAHS.2.36.

[151] K.L. McCloud III, L.P. Hall, J.A. Brady, Full-Scale Wind Tunnel Tests of Blowing Boundary Layer Control Applied to a Helicopter Rotor, Technical Report NASA TN D-335, 1960.

[152] K. Richter, H. Rosemann, Numerical investigation on the aerodynamic effect of mini-TEDs on the AWIATOR aircraft at cruise conditions, in: 25th International Congress of the Aeronautical Sciences, Hamburg, Germany, 2006.

[153] Y.H. Yu, S. Lee, K.W. McAlister, C. Tung, C.M. Wang, Dynamic stall control for advanced rotorcraft application, AIAA J. 33 (2) (1995) 289–295, http://dx.doi.org/10.2514/3.12496.

[154] L.W. Carr, M.S. Chandrasekhara, M.C. Wilder, K.W. Noonan, Effect of compressibility on suppression of dynamic stall using a slotted airfoil, J. Aircr. 38 (2) (2001) 296–309, http://dx.doi.org/10.2514/2.2762.

[155] S.A. Prince, V. Khodagolian, Low-speed static stall suppression using steady and pulsed air-jet vortex generators, AIAA J. 49 (3) (2011) 642–654, http://dx.doi.org/10.2514/1.J050754.

[156] S. Kota, G. Ervin, R. Osborn, R.A. Ormiston, Design and Fabrication of an Adaptive Leading Edge Rotor Blade, in: American Helicopter Society 64th Annual Forum, Montreal, Canada, 2008.

[157] W. Geissler, M. Raffel, Dynamic Stall Control by Airfoil Deformation, in: 19th European Rotorcraft Forum, Cernobbio, Italy, 1993.

[158] F. Samara, D.A. Johnson, Deep dynamic stall and active aerodynamic modification on a S833 airfoil using pitching trailing edge flap, Wind Eng. 45 (4) (2021) 884–903, http://dx.doi.org/10.1177/0309524X20938858.

[159] F. Samara, D.A. Johnson, Dynamic Stall on Pitching Cambered Airfoil with Phase Offset Trailing Edge Flap, AIAA J. 58 (7) (2020) 2844–2856, http://dx.doi.org/10.2514/1.J059115.

[160] P. Gerontakos, T. Lee, Dynamic stall flow control via a trailing-edge flap, AIAA J. 44 (3) (2006) 469–480, http://dx.doi.org/10.2514/1.17263.

[161] P. Crozier, P. Leconte, Y. Delrieux, B. Gimonet, A. Le Pape, H. Mercier de Rochettes, Wind-tunnel tests of a helicopter rotor with active flaps, in: 32nd European Rotorcraft Forum, Maastricht, Netherlands, 2006.

[162] A. Rabourdin, J. Maurice, O. Dieterich, P. Konstanzer, Blue Pulse Active Rotor Control at Airbus Helicopters—New EC145 Demonstrator and Flight Test Results, in: American Helicopter Society 70th Annual Forum, Montreal, Canada, 2014.

[163] M.P. Kinzel, M.D. Maughmer, E.P.N. Duque, Miniature Trailing-Edge Effectors for Rotorcraft Performance Enhancement, J. Am. Helicopter Soc. 52 (2) (2007) http://dx.doi.org/10.4050/JAHS.52.146.

[164] M. Khoshlahjeh, F. Gandhi, Extendable chord rotors for helicopter envelope expansion and performance improvement, J. Am. Helicopter Soc. 59 (1) (2014) 1–10, http://dx.doi.org/10.4050/JAHS.59.012007.

[165] R.H. Liebeck, Design of subsonic airfoils for high lift, J. Aircr. 15 (9) (1978) 547–561, http://dx.doi.org/10.2514/3.58406.

[166] E. Gruschwitz, O. Schrenk, Über eine Einfache Möglichkeit zur Auftriebserhöhung von Tragflügeln, Z. Flugtechnik Motorluftschiffahrt 23 (20) (1932) 597–601.

[167] E.F. Zaparka, Aircraft and control thereof, U.S. Patent No. Re19412, 1935.

[168] K. Richter, H. Rosemann, Steady aerodynamics of miniature trailing-edge devices in transonic flows, J. Aircr. 49 (3) (2012) 898–910, http://dx.doi.org/10.2514/1.C031563.

[169] A. Zanotti, G. Gilbertini, Experimental assessment of an active L-shaped tab for dynamic stall control, J. Fluids Struct. 77 (2018) 151–169, http://dx.doi.org/10.1016/j.jfluidstructs.2017.11.010.

[170] S. Barbarino, F. Gandhi, S.D. Webster, Design of extendable chord sections for morphing helicopter rotor blades, J. Intell. Mater. Syst. Struct. 22 (9) (2011) 891–905, http://dx.doi.org/10.1177/1045389X11414077.

[171] C.C. Wolf, A.D. Gardner, C.B. Merz, S. Opitz, Influence of a back-flow flap on the dynamic stall flow topology, CEAS Aeronaut. J. 9 (11) (2018) 39–51, http://dx.doi.org/10.1007/s13272-017-0274-z.

[172] A.W. Lang, M.T. Bradshaw, J.A. Smith, J.N. Wheelus, P.J. Motta, M.L. Habegger, R.E. Hueter, Movable Shark Scales Act as a Passive Dynamic Micro-Roughness to Control Flow Separation, Bioinspiration Biomim. 9 (3) (2014) 036017, http://dx.doi.org/10.1088/1748-3182/9/3/036017.

[173] G. Bramesfeld, M.D. Maughmer, Experimental Investigation of Self-Actuating, Upper-Surface, High-Lift-Enhancing Effectors, J. Aircr. 39 (1) (2002) 120–124, http://dx.doi.org/10.2514/2.2905.

[174] C. Brücker, C. Weidner, Separation control via self-adaptive hairy flaplet arrays, in: ERCOFTAC International Symposium -Unsteady Separation in Fluid-Structure Interaction, Mykonos, Greece, 2013.

[175] D.W. Bechert, M. Bruse, W. Hage, R. Meyer, Biological surfaces and their application: Laboratory and flight experiments on drag reduction and separation control, in: AIAA–1997–1960, AIAA 28th Fluid Dynamics Conference, Snowmass Village, CO, U.S.A., 1997, http://dx.doi.org/10.2514/6.1997-1960.

[176] G. Patone, W. Müller, Aeroflexible Oberflächenklappen als Rückstrombremsen nach dem Vorbild der Deckfedern des Vogelflügels, Engl: Aeroflexible surface flaps as reverse-flow brakes, modelled after the pop-up feathers of a bird, Technical Report TU Berlin TR-96-05, 1996.

[177] R.K.J. Meyer, Experimentelle Untersuchungen von Rückstromklappen auf Tragflügeln zur Beeinflussung von Strömungsablösungen, Engl: Experimental investigation of back-flow flaps on wings for the control of flow separation (Ph.D. thesis), TU Berlin, Germany, 2000.

[178] A.D. Gardner, S. Opitz, C.C. Wolf, C.B. Merz, Reduction of dynamic stall using a back-flow flap, CEAS Aeronaut. J. 8 (2) (2017) http://dx.doi.org/10.1007/s13272-017-0237-4.

[179] C. Zhu, Y. Qiu, Y. Feng, T. Wang, H. Li, Combined effect of passive vortex generators and leading-edge roughness on dynamic stall of the wind turbine airfoil, Energy Convers. Manage. (2021) http://dx.doi.org/10.1016/j.enconman.2021.115015.

[180] D. De Tavernier, C. Ferreira, A. Viré, B. LeBlanc, S. Bernardy, Controlling dynamic stall using vortex generators on a wind turbine airfoil, Renew. Energy 172 (2021) 1194–1211, http://dx.doi.org/10.1016/j.renene.2021.03.019.

[181] H. Mai, G. Dietz, W. Geissler, K. Richter, J. Bosbach, H. Richard, K. de Groot, Dynamic stall control by leading edge vortex generators, J. Am. Helicopter Soc. 53 (1) (2008) http://dx.doi.org/10.4050/JAHS.53.26.

[182] B. Heine, K. Mulleners, G. Joubert, M. Raffel, Dynamic stall control by passive disturbance generators, AIAA J. 51 (9) (2013) 2086–2097, http://dx.doi.org/10.2514/1.J051525.

[183] M.J. Smith, A.D. Gardner, R. Jain, D. Peters, F. Richez, Rotating Wing Dynamic Stall: State of the Art and Future Directions, in: American Helicopter Society 76th Annual Forum, Virginia Beach, VA, 2020.

[184] A. Le Pape, M. Costes, F. Richez, G. Joubert, F. David, J.M. Deluc, Dynamic stall control using deployable leading-edge vortex generators, AIAA J. 50 (10) (2012) http://dx.doi.org/10.2514/1.J051452.

[185] K. Al-Jaburi, D. Feszty, Passive flow control of dynamic stall via surface-based trapped vortex generators, J. Am. Helicopter Soc. 63 (3) (2018) 1–14, http://dx.doi.org/10.4050/JAHS.63.032005.

[186] W.F.J. Olsman, J.F.H. Willems, A. Hirschberg, R.R. Trieling, T. Colonius, Flow around a NACA0018 airfoil with a cavity and its dynamical response to acoustic forcing, Exp. Fluids 51 (2011) 493–509, http://dx.doi.org/10.1007/s00348-011-1065-7.

[187] M.L. Post, T.C. Corke, Separation Control Using Plasma Actuators—Dynamic Stall Vortex Control on an Oscillating Airfoil, AIAA J. 44 (12) (2006) 3125–3135, http://dx.doi.org/10.2514/1.22716.

[188] F.O. Thomas, T.C. Corke, M. Iqbal, A. Kozlov, D. Schatzman, Optimization of dielectric barrier discharge plasma actuators for active aerodynamic flow control, AIAA J. 47 (9) (2009) 2169–2178, http://dx.doi.org/10.2514/1.41588.

[189] G. Correale, I.B. Popov, A.E. Rakitin, A.Y. Starikovskii, S.J. Hulshoff, L.L.M. Veldhuis, Flow Separation Control on Airfoil with Pulsed Nanosecond Discharge Actuator, in: AIAA–2011–1079, 49th AIAA Aerospace Sciences Meeting and Exhibit, Orlando, FL, 2011, http://dx.doi.org/10.2514/6.2011-1079.

[190] A.J. Lombardi, P.O. Bowles, T.C. Corke, Closed-Loop Dynamic Stall Control Using a Plasma Actuator, AIAA J. 51 (5) (2013) 1130–1141, http://dx.doi.org/10.2514/1.J051988.

[191] G. Zhao, Y. Huang, Y. Yang, G. Li, H. Yang, Dynamic stall control over a rotor airfoil based on AC DBD plasma actuation, Adv. Aerodyn. 3 (1) (2021) http://dx.doi.org/10.1186/s42774-021-00061-2.

[192] H. Yang, H. Liang, G. Zhao, B. Wang, S. Zhang, W. Kong, Experimental study on dynamic stall control based on AC-DBD actuation, Plasma Sci. Technol. 23 (11) (2021) http://dx.doi.org/10.1088/2058-6272/ac1395.

[193] A. Séraudie, G. Pailhas, SIMCOS - Experimental Investigation on Static and Dynamic Stall with a Leading Edge Plasma Actuator, in F2 Wind Tunnel, Onera Technical Report RT 1/18164 DAAP/DMA, 2011.

[194] T. De Troyer, D. Hasin, D. Keisar, S. Santra, D. Greenblatt, Plasma-based dynamic stall control and modeling on an aspect-ratio-one wing, AIAA J. 60 (5) (2021) 1–11, http://dx.doi.org/10.2514/1.J060933.

[195] D. Greenblatt, E.A. Whalen, I.J. Wygnanski, Introduction to the Flow Control Virtual Collection, AIAA J. 57 (8) (2019) 3111—3114, http://dx.doi.org/10.2514/1.J058507.

[196] Y. Tan, T.M. Crittenden, A. Glezer, Aerodynamic Control of a Dynamically Pitching VR-12 Airfoil using Discrete Pulsed Actuation, in: AIAA–2016–0321, 52nd Aerospace Sciences Meeting, AIAA SciTech 2014, San Diego, CA, 2016, http://dx.doi.org/10.2514/6.2016-0321.

[197] J. Kearney, A. Glezer, Aerodynamic control of a pitching airfoil by active bleed, in: AIAA–2014–2045, 32nd AIAA Applied Aerodynamics Conference, Atlanta, GA, 2014, http://dx.doi.org/10.2514/6.2014-2045.

[198] B. Wake, E.A. Lurie, Computational Evaluation of Directed Synthetic Jets for Dynamic Stall Control, in: Proceedings of the 57th Annual American Helicopter Society Forum, Washington, DC, 2001.

[199] C.G. Matalanis, P.O. Bowles, B.Y. Min, S. Jee, A.E. Kuczek, B.E. Wake, P.F. Lorber, T.M. Crittenden, A. Glezer, N.W. Schaeffler, High-Speed Experiments on Combustion-Powered Actuation for Dynamic Stall Suppression, AIAA J. 55 (9) (2017) 3001–3015, http://dx.doi.org/10.2514/1.J055700.

[200] D. Greenblatt, I. Wyganski, Dynamic stall control by periodic excitation, part 1: NACA0015 parametric study, J. Aircr. 38 (3) (2001) 430–438, http://dx.doi.org/10.2514/2.2810.

[201] A. Seifert, A. Darabi, I. Wygnanski, Delay of airfoil stall by periodic excitation, J. Aircr. 33 (4) (1996) http://dx.doi.org/10.2514/3.47003.

[202] B. Nishri, I. Wygnanski, Effects of periodic excitation on turbulent separation from a flap, AIAA J. 36 (4) (1998) 547–556, http://dx.doi.org/10.2514/2.428.

[203] D. Weaver, K.W. McAlister, J. Tso, Control of VR7 dynamic stall by strong steady blowing, J. Aircr. 41 (6) (2004) 1404–1413, http://dx.doi.org/10.2514/1.4413.

[204] A.D. Gardner, K. Richter, H. Mai, D. Neuhaus, Experimental investigation of high-pressure pulsed blowing for dynamic stall control, CEAS Aeronaut. J. 5 (2) (2014) http://dx.doi.org/10.1007/s13272-014-0099-y.

[205] A.D. Gardner, K. Richter, H. Mai, D. Neuhaus, Experimental investigation of air jets for the control of compressible dynamic stall, J. Am. Helicopter Soc. 58 (4) (2013) http://dx.doi.org/10.4050/JAHS.58.042001.

[206] T.M. Crittenden, G.T. Woo, A. Glezer, Combustion-Powered Actuation for Transitory Flow Control, AIAA J. 56 (9) (2018) 3414–3435, http://dx.doi.org/10.2514/1.J056783.

[207] C.G. Matalanis, B.Y. Min, P.O. Bowles, S. Jee, B.E. Wake, T.M. Crittenden, G. Woo, A. Glezer, Combustion-Powered Actuation for Dynamic-Stall Suppression: High-Mach Simulations and Low-Mach Experiments, AIAA J. 53 (8) (2015) http://dx.doi.org/10.2514/1.J053641.

[208] J. Yen, N.A. Ahmed, Parametric Study of Dynamic Stall Flow Field With Synthetic Jet Actuation, J. Fluids Eng. 134 (7) (2012) 071106, http://dx.doi.org/10.1115/1.4006957.

[209] L.W. Traub, A. Miller, O. Rediniotis, Effects of synthetic jets on large-amplitude sinusoidal pitching motions, J. Aircr. 42 (1) (2005) 2844–2856, http://dx.doi.org/10.2514/1.3919.

[210] H. Nagib, J. Kiedaisch, D. Greenblatt, I. Wygnanski, A. Hassan, Effective flow control for rotorcraft applications at flight Mach numbers, in: AIAA–2001–2974, 15th AIAA Computational Fluid Dynamics Conference, 2001, http://dx.doi.org/10.2514/6.2001-2974.

[211] M.J. Smith, A.R. Jones, F. Ayancik, K. Mulleners, J.W. Naughton, An Assessment of the State-of-the-Art from the 2019 ARO Dynamic Stall Workshop, in: AIAA-2020-2697, AIAA Aviation Forum, 2020, http://dx.doi.org/10.2514/6.2020-2697, Virtual.

[212] M. Ramasamy, R. Jain, T.R. Norman, Does Scatter Matter? Improved Understanding of UH-60A Wind Tunnel Rotor Measurements Using Data-Driven Clustering and CREATE-AV Helios, in: Proceedings of the 77th Annual Forum, The Vertical Flight Society, 2021, Virtual.

[213] M. Ramasamy, J.S. Wilson, W.J. McCroskey, P.B. Martin, Characterizing cycle-to-cycle variations in dynamic stall measurements, J. Am. Helicopter Soc. 63 (2) (2018) 1–24, http://dx.doi.org/10.4050/JAHS.63.022002.